THEMA

théorie économique, modélisation et applications

THEMA Working Paper n°2024-10
CY Cergy Paris Université, France

Speeding Towards Cleaner Air: An Evaluation of Maximum Speed Restrictions in Île-de-France during High Pollution Days

Romuald Le Frioux, André de Palma, Nadège Blond

September 2024

CY CERGY PARIS UNIVERSITÉ

cnrs

Speeding Towards Cleaner Air: An Evaluation of Maximum Speed Restrictions in Île-de-France during High Pollution Days

R. Le Frioux[†], A. de Palma[†], N. Blond[‡]

† *CY Cergy Paris Université and ThEMA*

‡ *Université de Strasbourg, CNRS, Laboratoire Image Ville Environnement, UMR7362, Strasbourg, France*

ABSTRACT: *This study explores how speed limit regulations for cars in Île-de-France affect air pollution from road traffic and the economic costs linked to the population's exposure to this pollution. Using an enhanced version ofthe comprehensive and integrative modeling system, METRO-TRACE (Le Frioux, de Palma, and Blond, 2023), the research combines detailed geographical data, a mobility model to simulate population movements, and an air quality model to assess the economics costs associated with population exposure to road traffic related air pollution . The findings show that the yearly cost of population exposure to road traffic pollution is 118.6 € per person. Implementing speed limit policies may not significantly reduce these costs unless they are substained over the long term or accompanied by behavioral adjustments. The study highlights the intricate relationship between speed limits, pollutant emissions, and their economic consequences.*

Key words: Traffic pollution, population exposure, integrated chain of model, dynamic transport model, air pollution exposure monetarization

JEL: R48 - Q51 - Q58 - Q53

Acknowledgment: The authors thank the participants of the CY Paris Cergy Université Urban and Transport seminar, the internal seminars, and specifically acknowledge Javaudin Lucas, Ghoslya Samarth, Lindsey Robin, Chapelle Guillaume, and Riou Yannik for their feedback. They also extend their gratitude to attendees of the 2023 and 2024 International Transport Economics Association and AICC conferences, as well as the 2024 International Conference on Sustainability, Environment, and Social Transition in Economics and Finance. The authors are grateful to MAAT and AFFINITE (Projet-ANR-20-CE22-0014) for their financial support.

1 Introduction

Air pollution poses significant environmental and health challenges, with global warming and direct impacts on well-being. Over 99% of the world's population exceeds recommended health protection levels, leading to 7 million premature deaths annually worldwide.[1] Urban areas exhibit diverse and high levels of air pollution (Dons et al., 2011; Hatzopoulou and Miller, 2010; Hatzopoulou, Hao, and Miller, 2011; Dhondt et al., 2012; Lefebvre et al., 2013; Rowangould, 2015; Vallamsundar et al., 2016). Several studies detail the impacts of air pollution on health outcomes in several cities (Garrett and Casimiro, 2011; Bañeras et al., 2018; Fang et al., 2016).

The health impacts of air pollution entail substantial social costs, with studies estimating billions in economic expenses associated with pollutants like PM and NO_2 for cities (Walton et al., 2015; Vlachokostas et al., 2012; Martinez et al., 2018). A comprehensive analysis of 432 European cities in 30 countries by de Bruyne and de Vries (2020) revealed that the cost of population exposure in France was approximately 10,979 millions euros[2] representing on average 770.4 euros per inhabitants, emphasizing the significant economic burden, particularly from PM, O_3 and NO_2.

Road transportation emerges as a significant contributor to air pollution, presenting a substantial public health concern due to heightened exposure near roads and the prevalent use of cars for commuting (McCubbin and Delucchi, 2003). Globally, the transportation sector, as reported by the International Energy Agency, accounts for about one-quarter of total energy-related CO_2 emissions, with the European transport sector responsible for 27% of GHG emissions in 2017 (22% excluding international aviation and maritime emissions).

According to the European Environment Agency's 2020 estimates reveal that road transportation contributes to approximately 70% of the total emissions in the European transportation sector, encompassing 37% of NO_x emissions, 18% of CO emissions, and 9% of $PM_{2.5}$ emissions.[3] Furthermore, chronic exposure to air pollution from PM and NO_2 originating from

[1] https://www.who.int/health-topics/air-pollutiontab=tab$_1$

[2] The cost is computed for the 76 biggest French cities

[3] https://www.eea.europa.eu/publications/air-quality-in-europe-2022/sources-and-emissions-of-air

road traffic is estimated to have led to over 70,000 premature deaths in the EU-27 in 2018, out of a total of 300,000 premature deaths attributed to overall air pollution. Notably, individuals residing in densely populated areas bear a disproportionate burden of these health impacts.[4]

The first objective of the paper is to present the new version of METRO-TRACE and its application Île-de-France[5], France. METRO-TRACE (METROPOLIS - Road-trafic Related Exposition Costs Evaluation) is an integrated chain of chain of models that enables the coherent prediction of trafic volume, speed, and flow on roads, estimation of pollutant emissions from vehicles, forecasting of pollutant dispersion in the air, estimation of the population exposure to air pollution, and the economic costs associated with it. The new version of METRO-TRACE has been updated to address speci c areas of improvement. These include the utilization of the latest edition of METROPOLIS2 (Javaudin and de Palma, 2024) and an enhancement of our emission model to account for a wider variety of vehicle types. The emission model can now compute emissions for each agent and each link. Our dispersion model has also been reconstructed to allow for dispersion calculations using spatially distributed wind speed and direction, while basic chem-ical transformation has been introduced to the model. Furthermore, we have added a module to our exposition model that enables the computation of exposure during the commuting process. Finally, the monetarization module has been rebuilt to provide more precise estimations. We focus on five pollutants carbon dioxide (CO_2), nitrogen oxides (NO_x), carbon monoxide (CO), Ozone (O_3), and particulate matter ($PM_{2.5}$). Applied to Île-de-France, the new approach aims to provide a comprehensive understanding of the impact of road traffic on air pollution in Île-de-France.

Second, the paper aims to assess the effectiveness of speed limitations policy implemented in Île-de-France during high pollution days. The proposed chain of models will be applied to analyze the mechanisms of speed limitations policy and evaluate its effectiveness in reducing the emission of pollutants and the associated costs of population exposure to air pollution. The study aims to provide a detailed costs-benefits analysis of the impact of speed limitations. By understanding the impact of speed limitations policy on air quality in Île-de-France and

[4]https://ec.europa.eu/commission/presscorner/detail/en/qanda$_2 2_6$496

[5]The region of Paris

its potential to improve the health and well-being of the local population. But also, potential welfare losses created by the increase of travel time or congestion.

In this paper, we have organized the content into seven sections. Section 2 provides an overview of non-technical measures that have been previously studied. Section 3 presents the METRO-TRACE integrated chain of models in detail. Section 4 introduces and describes the data that were used in our research. The application of this framework on Île-de-France (France) is presented in Section 5. In Section 6, we examine the effectiveness of speed limitations policy. Finally, Section 7 concludes the paper by presenting potential future research, limitations, and improvements

2 Literature review

2.1 Integrated chain of models to evaluate population exposure to road-traffic related air pollution

Several integrated chain models in the literature investigate the effects of road traffic on air pollution, notably in metropolitan settings. Despite a common focus on air pollution, these models differ in their methodologies and results, allowing for a more complete knowledge of road traffic's influence on air quality and offering insights for potential mitigation policies.

Initially, certain systems use traffic count data rather than traffic simulation models (Carslaw and Beevers, 2002; Cesaroni et al., 2012). The traffic simulation models enable dynamic simulations and policy evaluations, requiring validation using observed data. Most studies use emission and dispersion models and/or air quality model to assess population exposure to road traffic pollutants and analyze policy impact on pollution by examining changes in traffic patterns (de Nazelle, Rodríguez, and Crawford-Brown, 2009; Dons et al., 2011; Kickhöfer and Kern, 2015; Dias, Tchepel, and Antunes, 2016; Smith et al., 2016; Gurram, Stuart, and Pinjari, 2019; Etuman et al., 2020; Host et al., 2020; Lu, 2021; Poulhès and Proulhac; 2021; Naqvi et al., 2023).

Once pollutant concentrations are calculated, they are integrated into a population movement model to assess exposure, considering significant variations between living and working places and avoiding measurement errors in population exposure (de Nazelle, Rodríguez, and Crawford-Brown, 2009; Dons et al., 2011; Kickhöfer and Kern, 2015; Smith et al., 2016; Gurram, Stuart, and Pinjari, 2019; Etuman et al., 2020; Lu, 2021; Poulhès and Proulhac; 2021; Naqvi et al., 2023).

Only a limited number of studies have successfully integrated the road traffic, emissions, air quality, population movements, exposure, and also costs, as proposed by Kickhöfer and Kern (2015) in order to evaluate the monetary impact of policies on road traffic to assess potential costs and benefits. Due to computational efficiency concerns, the methods for pollutant dispersion and monetization relies on a simplified box model, neglecting factors such as wind speed, direction, atmospheric stability, and chemical processes. The new version of METRO-TRACE (Le Frioux, de Palma, and Blond, 2023) continues to address some of these issues as it takes into account pollutants dispersion, chemical equilibrium of O_3, NO, and NO_2, as well as population exposure during commuting processes.

2.2 French regulation concerning high air pollution events

The legal basis for the implementation of speed limit restrictions during high pollution days in France can be found in Joint Ministerial Decision of the 7^{th} april 2016[6]. This decree allows local authorities to take action to protect public health and the environment in the event of an air pollution peak, including the implementation of temporary measures such as speed limit reductions. This law is defined as follows: "All speed limits can be reduced by 20 $km.h^{-1}$ with a minimum speed limit of 70 $km.h^{-1}$". In accordance with the article R. 221-1 of environment code (Code de l'Environnement)[7] high pollution peak are defined when measured pollutant concentration for SO_2 and when estimated concentration for NO_x, O_3, and PM_{10} exceed regulatory thresholds.

Measures can be taken if those thresholds are exceeded for area larger than 100 km^2 and/or

[6] Arrêté interministériel du 7 avril 2016 relatif au déclenchement des procédures préfectorales en cas d'épisodes de pollution de l'air ambiant

[7] https://www.legifrance.gouv.fr/codes/article$_lc/LEGIARTI$000022964539

Table 1: Regulatory thresholds defining a high pollution day. Source: Article R. 221-1 of the French environment code

Pollutants	Concentration threshold
NO_2	400 µg.m^{-3} during 3 successive hours and/or 200 µg.m^{-3} during more than 2 successive days
PM_{10}	80 µg.m^{-3} in daily mean
SO_2	500 µg.m^{-3} during 3 successive hours
O_3	340 µg.m^{-3} during 3 successive hours

if more than 20% of the population of département is exposed for those with population higher than 500,000 inhabitants and if more than 50,000 inhabitants are exposed for others. Notice that for SO_2 the overtaking of the threshold on at least one air control station is sufficient.

Typically, such occurrences are observed in December, primarily as a result of an overabundance of particulate matter (PM) caused by increased domestic heating, and in March, April, by increased agricultural activites and ammonia emissions.

3 METRO-TRACE: An integrated chain of models to evaluate impacts of road transport policy on air pollution

Bringing together diverse data and models, an integrated chain provides a comprehensive perspective, with each component supplying unique information. This unified model chain is crafted to yield cohesive insights into traffic patterns, vehicle speeds, air pollutant emissions, public exposure to air pollution, and the associated costs. Additionally, it provides valuable guidance for shaping decisions and policies aimed at reducing emissions and improving air quality. We opted to integrate the monetarization model into the chain as it allows for standardizing all elements in euros, facilitating a complete cost-benefit analysis of a project or policy. In this chapter, we update the latest version of METRO-TRACE (Le Frioux, de Palma, and Blond, 2023). Figure 2.1 illustrates the structure of this integrated model chain, and subsequent sections delve into the specifics of each model.

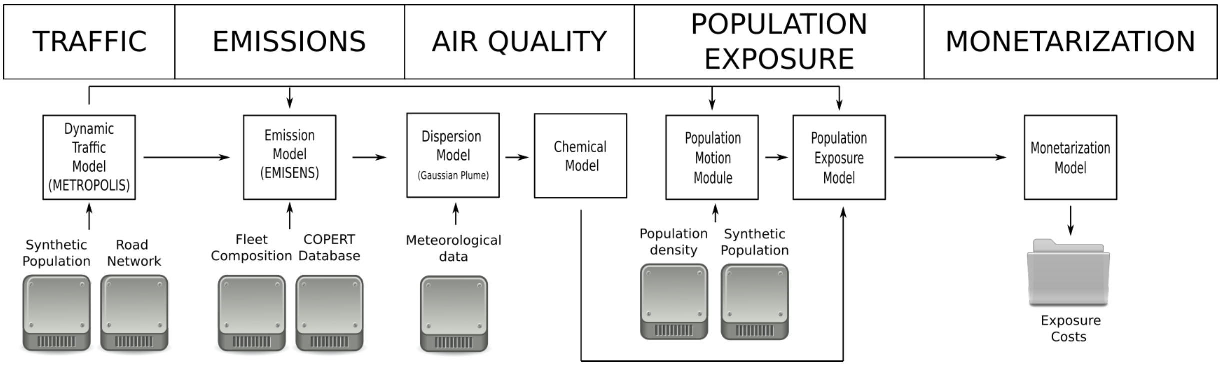

Figure 1: Structure of METRO-TRACE (Traffic Related Air pollution Costs Evaluation)

3.1 Road traffic model

We choose to use METROPOLIS2 (Javaudin and de Palma, 2024) to compute and evaluate road traffic. As it is a dynamic, mesoscopic[8] traffic simulator that treats agent-level endogenous options for modes, departures times, and routes. Therefore, this allows us to explore a wider range of scenarios and policies that could impact pollutant emissions and population exposure to air pollution.

METROPOLIS2 is assuming that every agent has a cost associated with its preferences for their trip. This cost is expressed as a function of two components: the deviation from the preferred trip duration and the one from the preferred arrival time. This preferences are based on the fact that travellers prefer to arrive at their destination as close as possible to their preferred arrival time in order to minimize their travel costs. These preferences are based on the Vickrey (1969) approach and can be summarized by the following formula:

$$C_A(\tau) = c_m + \alpha_m T(\tau) + \beta max[t^* - \tau - T(\tau); 0] + \gamma max[\tau + T(\tau) - t^*; 0]$$

where, $C_A(\tau)$ is the cost of departing at time τ (in €), t^* is the desired arrival time (in h), c_m is the cost from taking transportation mode m (in €.h^{-1}), $T(\tau)$ is the travel time for a departure at time τ (in h), α_m is the unit cost of travel time from taking transportation mode m (in €.h^{-1}), β and γ are respectively the unit costs of arriving early and late (in €.h^{-1}).

[8] In that it is neither microscopic nor macroscopic, it is mesoscopic. This model nonetheless simulates flows, speed, and congestion at the link level even though it does not simulate acceleration or traffic stops.

According to a learning process that considers the situation seen over the previous days, agents revise their mode choice, departure time, and route decision at each iteration (de Palma and Marchal; 2002). As a consequence of this procedure, the simulation reaches a stable state. The model represents congestion through bottleneck congestion (Arnold et al.; 2004). It presupposes that congestion arises when the volume of vehicles approaching the bottleneck exceeds its capacity. This situation compels travelers to wait until they can pass through, leading to expanded travel times and diminished efficiency.

3.2 Emission model

Our emission model relies on the European EMEP/EA reglementation. It is an upgraded version of EMISENS model (Le Frioux, de Palma, and Blond, 2023; Ho, Clappier, and Blond, 2014). It can be classified as a mesoscopic emission model (as defined by Smit, Ntziachristos, and Boulter, 2010) that computes emissions factors by using emission factors considering the average speed on each link and for each agent according to their type of vehicle. This model uses average speed, ambient outdoor temperature, and traffic volume to generate emissions for four types of pollutants (in g): carbon dioxide (CO_2), particulate matter with diameter lower than 2.5 μm ($PM_{2.5}$), nitrogen oxide (NO_x) and carbon monoxide (CO) as well as the fuel consumption (FC). It computes hot and cold (excess emissions from cold engine) emissions from the exhaust pipe as well as non-exhaust emissions, such as emissions from tyre wear, brake wear and road abrasions.

The hot emission factors (in $g.km^{-1}$), $e_k^{hot}[S_n(r_i,t),v]$ of pollutant k (CO_2, $PM_{2.5}$, NO_x, CO) has been restrived from the 2019 COPERT database (Ntziachristos et al., 2009) for each type of vehicle v as a function of the average speed of agent n, $S_n(r_i,t)$ on entering on directed road r_i at time t. Average emissions factors $\overline{e_k}^{hot}[S_n(r_i,t),l]$ for each Vignette Crit'air l are computed based on the fleet composition using the CITEPA's 2019 data resulting in ten different vehicles classes. The quantity of pollutant k emitted (in g) by agent n with vehicle class l entering on directed road r_i at time t, considering warm engines, $E_k^{hot}(r_i,t,n)$ (in g) is given by the following equation:

$$E_k^{hot}(r_i,t,n) = L(r_i) \times \overline{e_k^{hot}}[S_n(r_i,t),l_n],$$

where $L(r_i)$ is the length of directed road r_i (in km), and $\overline{e_k^{hot}}[S_n(r_i,t), l_n]$ (in $g.km^{-1}$) denotes the average hot emissions factors of vehicle of class l of agent n according to its average speed on directed road r_i for entering on the road at time t. Note that the average speed is unique for each individual, it is equal to the time to cross the link for an agent entering at specific time divided by the length of the road. This information enables us to calculate emissions not only at the road level but also at the individual agent level. Using average speed is not an issue in our case, as directed roads are relatively small (more than 75% of them are smaller than 150 meters). Furthermore, our emission factors somewhat account for the effects of acceleration.

The cold emissions (in g) are emissions to be added to the hot emissions in order to consider that at the beginning of their trip agents have cold engines. Cold emissions $E_k^{cold}(r_i,t,T,n)$ for pollutant k realesed by agent n, entering on directed road r_i at time t according to the outdoor temperature T are derived from the hot emissions using this equation:

$$E_k^{cold}(r_i,t,T,n) = E_k^{hot}(r_i,t,n) \times \frac{\overline{e_k^{cold}}[S_n(r_i,t),l_n,T]}{\overline{e_k^{hot}}[S_n(r_i,t),l_n]},$$

where $\overline{e_k^{cold}}[S_n(r_i,t),l_n,T]$ is the average cold emission factor for pollutant k, for outdoor temperature T (in celsius degree) according to the average speed $(S_n(r_i,t))$ for vehicle of class l of agent n when entering on directed road r_i at time t. Notice that cold emission are only computed for the first 11 kilometers of each trip.

The emission (in g) of pollutant k from tyre wear, brake wear, and road abrasion of agent n when entering on directed road r_i at time t, $E_k^{non-exhaust}(t,r_i,n)$ are computed as follows:

$$E_k^{non-exhaust}(t,r_i,n) = L(r_i) \times \left(e_k^{bw} f_k^{bw} \zeta_k^{bw}[S_n(r_i,t)] + e_k^{rs} f_k^{rs} \zeta_k^{rs}[S_n(r_i,t)] + e_k^{tw} f_k^{tw} \zeta_k^{tw}[S_n(r_i,t)]\right),$$

where e_k^{bw} (in $g.km^{-1}$) is the emission factor for emissions of total suspended particles (TSP) from brake wear and where f_k^{bw} (in %) is the mass fraction of TSP from brake wear attributable to pollutant k and $\zeta_k^{bw}[S_n(r_i,t)]$ is the speed correction factor for brake wear emissions according to the speed of agent n entering on the directed road r_i at time t, e_k^{rs} (in $g.km^{-1}$) is the emission factor for emissions of TSP from road surface and f_k^{rs} (in %) is the mass fraction of TSP from road surface wear attributable to pollutant k and $\zeta_k^{rs}[S_n(r_i,t)]$ is the speed correction factor for road surface wear emissions according to the speed of agent a entering on the directed road r_i at time t, and e_k^{tw} (in $g.km^{-1}$) is the emission factor for emissions of TSP from tyre wear and f_k^{tw} (in %) is the mass fraction of TSP from tyre wear attributable to pollutant k, and $\zeta_k^{tw}[S_n(r_i,t)]$ is the speed correction factor for tyre wear emissions according to the speed of agent n entering on the directed road r_i at time t.

Finally, the quantity of pollutant released during one second at emitter j during period of time h, $Q_k^j(h)$ is obtained using the following equation:

$$Q_k^j(h) = \sum_{t\in h}\sum_{n\in\mathcal{N}}\sum_{r_i\in I(j)} \epsilon^j(r_i)\times[E_k^{hot}(t,r_i,a)+E_k^{cold}(t,r_i,a)+E_k^{non-exhaust}(t,r_i,n)]\times 10^{-6}\times\Delta h^{-1},$$

where $\epsilon^j(r_i)$ is the proportion of the directed road r_i included in the cell of the emitter j, where Δh is the duration of the period h measures in seconds (here 3,600), $\mathcal{N}$ in the set of agents, and $I(j)$ is the set of directed roads crossing cell j.

3.3 Air quality model

A lot of different air quality models exist. They are characterized by their spatial and time resolutions, and their mathematical approach. These approaches are directly linked to the processes simulated, the extension of the domain and associated with computation performances. We choose to use Gausian plume model (Sutton, 1947) and focus on primary pollutants. Such a model does not compute the atmospheric dynamic and chemistry (and thus the production of secondary pollutants). However, it is able to estimate the dispersion of the air pollution due to the advection of air pollution by the wind and the air mixing due to turbulences, in an efficient manner. This model takes as inputs the air pollutant emissions, atmospheric stability parameters, wind direction and intensity, and compute the pollutant concentrations as follows:

$$C_k^i(h,(x(h),y(h),z)) = \frac{Q_k^j(h)}{2\pi u_s(h)\sigma_y(x(h))\sigma_z(x(h))}exp(\frac{-y(h)}{2\sigma_y(x(h))})[exp(\frac{-(z+H)}{2\sigma_z(x(h))})+exp(\frac{-(z-H)}{2\sigma_z(x(h))})],$$

where $C_k^i(h,(x(h),y,z))$ (in $\mu g.m^{-3}$) is the concentrations of pollutant k at receptor i with the Cartesian coordinates (x,y,z) during period h, where $x(h)$ is the downwind distance (in m) during period h, y the cross wind distance (in m) during period h, and z the receptor height (in m). $Q_k^j(h)$ is the quantity of pollutant k released at the emitter j (in $\mu g.s^{-1}$) during period h, $u_s(h)$ is the mean wind speed (in $m.s^{-1}$) during period h at the pollutant release height H (in m) and, $\sigma_y(x(h))$ and $\sigma_z(x(h))$ are the standard deviations of respectively lateral and vertical concentration distribution during period h, that are highly depend from the atmospheric stability conditions. Concentrations are computed for each hour using a grid of receptors with a definition of 100m. They mainly depend on the distance between the emitter (i.e, the place at which the pollutant is released) and a receptor, representing the different places where residents can be located.

Such dispersion model is only able to compute, primary pollutant dispersion. In order to take consider of the fast chemical reaction between NO_x and local tropospheric concentrations of O_3, a photochemical equilibrium reactions is considered. This equilibrium leads to a relation between O_3 and NO_x concentrations known as the Leighton ratio (Leighthon, 1961) at the photostationary steady state (PSS):

$$[O_3]_{PSS} = \frac{J_1[NO_2]_{PSS}}{k_3[NO]_{PSS}},$$

where $[O_3]_{PSS}$, $[NO_2]_{PSS}$, and $[NO]_{PSS}$ (in ppb) are respectively the O_3, NO_2, and NO concentrations at the photostationary steady state. The chemical rate constant k_3 (in pbb^{-1}/s) is the rate at which nitric oxide and ozone are transformed into nitrogen and dioxygen ($NO + O_3 \rightarrow NO_2 + O_2$). It is a first-order kinetic constant which can be computed as a function of the temperature T (in K) (Hanrahan, 1999). The photolysis rate coefficient J_1 (in s^{-1}) is the rate at which nitrogen dioxide is photolyzed into nitric oxide and oxygen ($NO_2 + hv \rightarrow NO + O$)[9]. Photolysis frequency, can be calculated by integrating a product involving the solar actinic flux for a given wavelength (Dickerson, Stedman, and Delany, 1982). According to Wiegand and Bofinger (2000), an alternative way based on empirical expressions does exist and the photolysis frequency can be computed as a function of the zenithal angle. In this chapter the ratio of the two constants ($\frac{J_1}{k_3}$) is calibrated in order to fit the background concentrations of O_3 when the concentrations of NO_2 and NO are null.

Our emission model is only able to compute emissions of NO_x. We use Romberg et al. function (Romberg et al., 1996) to compute the hourly concentrations of NO_2 in $\mu g.m^{-3}$ ($[NO_2]_h$) using the following formula:

$$[NO_2]_h = \frac{103 \times [NO_x]_h}{[NO_x]_h + 130} + 0.0005 \times [NO_x]_h,$$

[9] hv are photons

where $[NO_x]_h$ (in $\mu g.m^{-3}$) is the hourly concentrations of NO_x.

Given the chemical definition of NO_x, it is straighfoward to recover hourly NO concentrations in ppb ($[NO]_h$) using the following relationship:

$$[NO]_h = [NO_x]_h - [NO_2]_h.$$

In order to fit our modelization to the concentration observed in our studied areas, we need to calibrate the ratio of the two constant (J_1/k_3).

3.4 Population exposure-monetarization model

The monetary cost (in €) of population exposure of agent n in cell j during period h, $€_k^j(h,n)$ is computed as follows:

$$€_k^j(h,n) = \textit{time spend}^j(n,h) \times c_k(C_k^j(h)),$$

where c_k is the exposure costs function (in $€.h^{-1}$) to pollutant k with a concentration of $C_k^j(h)$ (in $\mu g.m^{-3}$) in cell j during period h and $\textit{time spend}^j(n,h)$ is the time spend (in h) by agent n during period h in cell j.

4 Data collection over Île-de-France (France) and treatments

4.1 Île-de-France

The Île-de-France region, categorized as NUTS-2 in the Eurostat classification, has over 12,250,000 residents, accounting for 18.8% of the total French population. This region, which has a population density of around 1,000 people per square kilometer, is even more significant because it is home of Paris, France's capital. Île-de-France has the highest GDP per capita in the country, at roughly 60,000 €.

4.2 Input data for traffic simulations

The model is specifically applied during morning hours, from 3 to 10 a.m. It makes use of agent characteristics from a synthetic population to provide extensive insights on travel demand, such as socio-demographic characteristics, personal residences, and people's daily activities (Hörl and Balac, 2021). The results come from a variety of open and publicly available datasets, including travel surveys, census surveys, and cadastral data.

Parameter	**Value**
Unit cost of travel time from taking car (α_{car})	10
Unit cost of travel time from walking (α_{walk})	10
Unit cost of travel time taking public transit (α_{public})	8
Constant cost from taking car (c_{car})	3
Constant cost from walking (c_{walk})	0
Constant cost from taking public transit (c_{public})	1.5
Unit cost of arriving early (β)	5
Unit cost of arriving late (γ)	5
Half-width of the on-time arrival window (Δ)	0

Table 2: METROPOLIS2 parameter cost values (in €.h^{-1})

Table 2.2 describes the different parameters values used for our METROPOLIS2 simulations.

METROPOLIS2 relies on a road network with 603,434 links, spanning a total distance of 72,562 kilometers across the studied area, as depicted in Figure 2.2. In this study, we used a simplified OpenStreetMap network. Notably, there is a concentrated density of links in Paris, gradually decreasing as we move away from the city.

The network has a maximum speed of 130 $km.h^{-1}$ with a minimum of 10 $km.h^{-1}$. A significant portion of the network imposes speed limits of 30 $km.h^{-1}$, 50 $km.h^{-1}$, or 80 $km.h^{-1}$, constituting 43%, 19%, and 16%, respectively. Notably, only 23% of the total network length is affected by the policy, indicating speed limits greater than 70 $km.h^{-1}$. Additionally, it is observed that the spatial density of these speed limits appears denser at the boundaries of the zone, gradually decreasing closer to Paris.

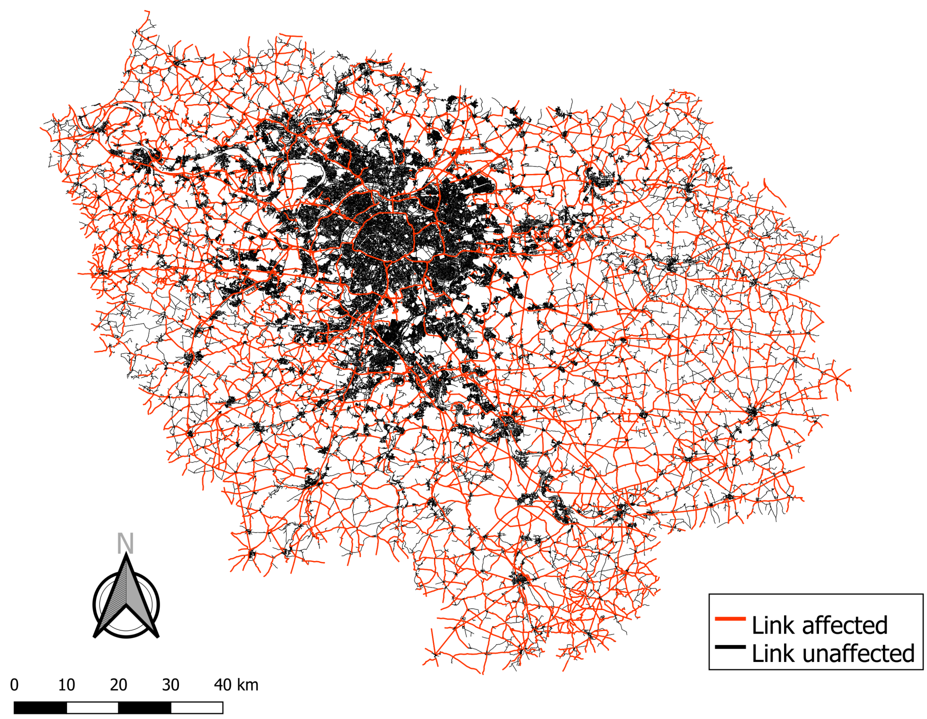

Figure 2: Road network of Île-de-France, with the links affected by the transport policy, indicating speed limits greater than $70km.h^{-1}$ Source: OpenStreetMap

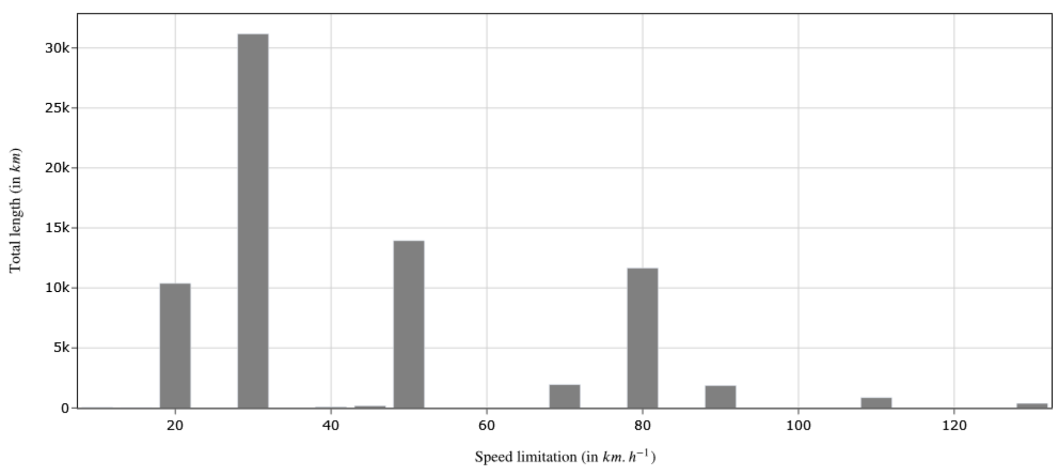

Figure 3: Density distribution total length of links per speed limit (in $km.h^{-1}$). Source: OpenStreetMap

4.3 Input data for emission simulations

Figure 2.4 illustrates the composition of the French vehicle fleet. Predominantly, diesel-powered passenger cars make up the majority, with a significant proportion adhering to the EURO 5 and EURO 6 European standards. However, a notable segment of the fleet, exceeding 20 years old and falling within EURO 1 and EURO 2 categories, is identified, known for elevated emissions levels. Addressing this portion should be prioritized in pollution mitigation efforts. Examining the car classes for Île-de-France, it is noteworthy that the majority falls into the categories of Diesel Crit'Air 3, Petrol Crit'Air 1, and Diesel Crit'Air 2.[10]

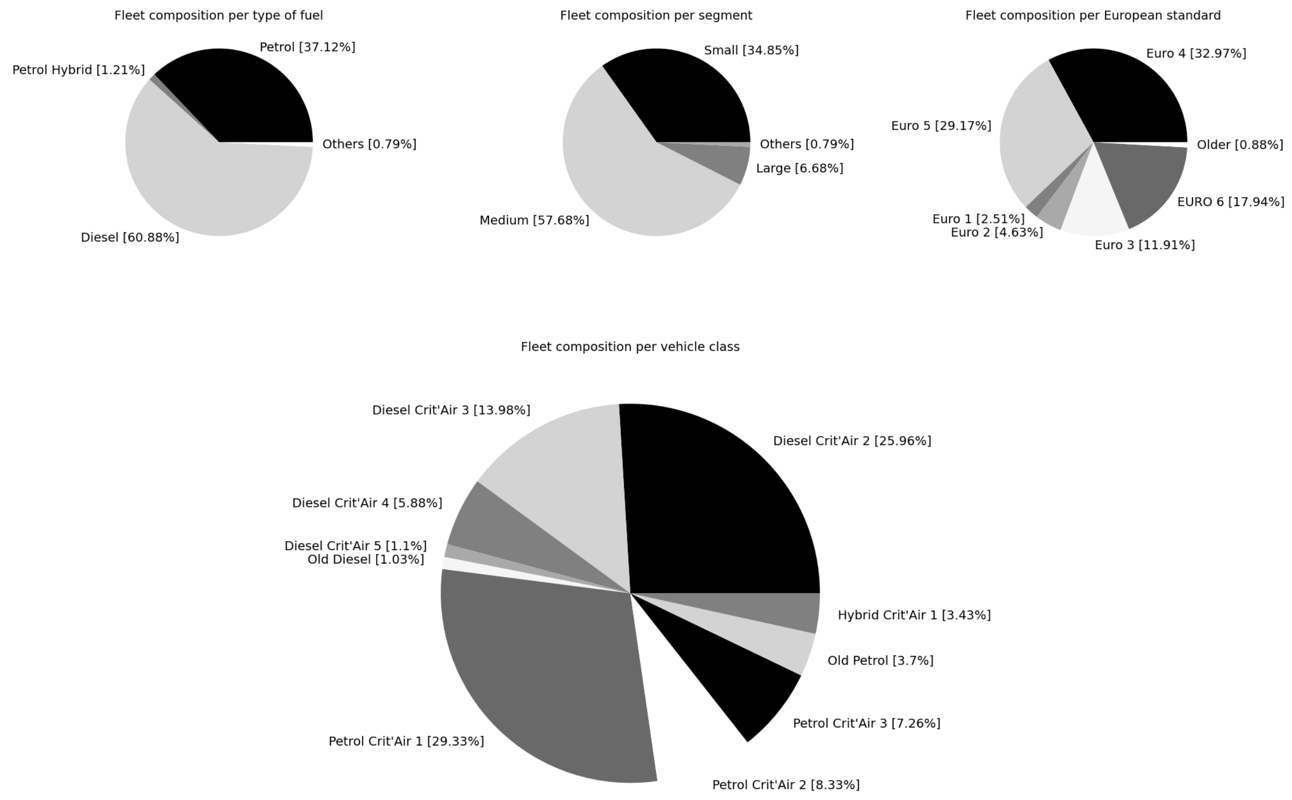

Figure 4: French fleet composition per motorization types, vehicle size, European standards, and vehicle class for Île-de-France. Source: CITEPA (2019) and French ministry of ecological transition and territorial cohesion

[10] A table of the correspondances between Crit'air reglementation and fuel types and Euro standard is available in Appendix

Figure 2.5 depicts air pollutant emissions from passenger cars across different vehicle classes. The average emission factor is computed considering the national fleet composition (CITEPA, 2019) and the emission factors from the COPERT III database (2019) for each vehicle type. Notably, these emission factors exhibit a minimum level at a speed of 65 $km.h^{-1}$. Vehicle engine emissions demonstrate a U-shaped and asymmetric curve concerning speed. At low speeds, such as in stop-and-go traffic, engines work harder for vehicle movement, resulting in inefficient fuel combustion and increased pollutant emissions. Conversely, at high speeds on highways, less efficient fuel combustion and heightened pollutant emissions occur. Increased aerodynamic drag at high speeds further contributes to emissions. At medium speeds, engines operate more efficiently, and lower aerodynamic drag results in reduced emissions. Specifically, CO emissions can vary by a factor of 3.5, while NO_x and CO_2 can vary by a factor of 2, and $PM_{2.5}$ can vary by a factor of 1.6. Emissions are computed on each link based on the mean speed calculated by METROPOLIS2, with expectations of higher emissions on low and high-speed links.

4.4 Input data for air pollutant concentration simulations

Air pollution concentrations are calculated at a spatial resolution of 100 m. The dispersion module initially interpolates vehicle emissions on a 100 m grid domain. Wind speed and direction data are sourced from two providers. The first source is the COPERNICUS climate in the city database (Hooyberghs et al., 2019). These data, with a spatial resolution of 100 meters, are generated using a sophisticated meteorological model, UrbClim, to consider urban meteorological intricacies, such as the canyon effect. However, these data are restricted to a specific area encompassing Paris and its surroundings. To compute dispersion for the entire Île-de-France, we complemented our data with the ERA5 (Hersbach et al., 2023) meteorological data where COPERNICUS data were unavailable. ERA5 have a resolution of $\sim 25km$.

Figure 2.6 presents the spatial distribution of wind speed from both sources in panel (a) and exclusively from COPERNICUS in panel (b). A notable observation is the higher wind speed in the bed of the Seine River compared to other locations. In panel (b), it is evident that ERA5 data shows lower wind speed values. However, it is important to highlight that by combin-

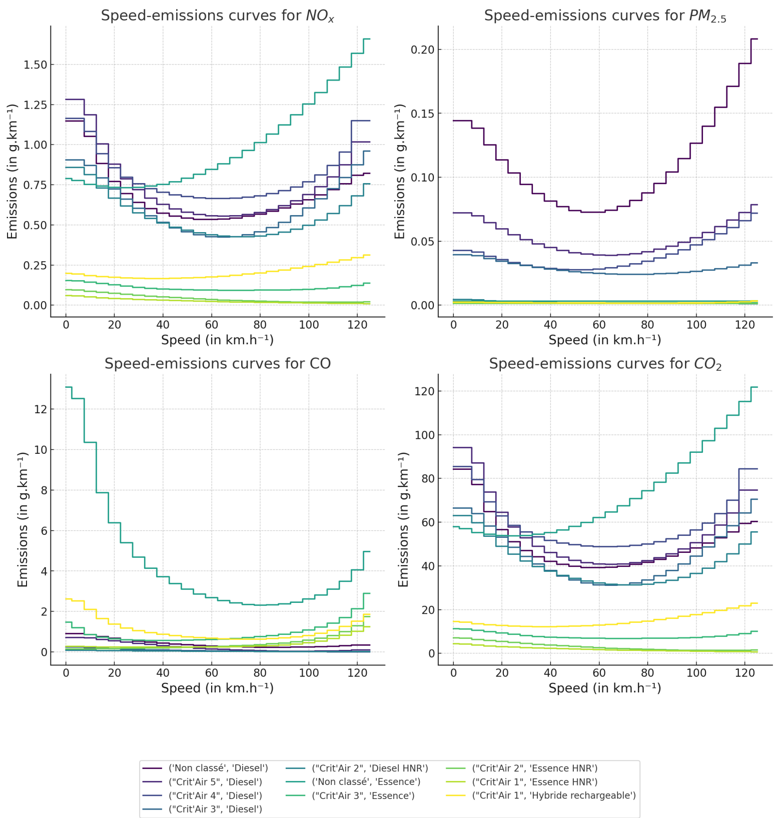

Figure 5: Hot mean emission factor (in $g.km^{-1}$) for each vehicle class as a function of speed (in $km.h^{-1}$), computed according to the national fleet composition. Sources: fleet composition (CITEPA, 2019) and emission factors (Ntziachristos et al., 2009)

ing both data sources, wind speed appears relatively uniform across the studied area, ranging between 1.02 and 3.3 $m.s^{-1}$. Additionally, all winds are consistently from the North-West, exhibiting an angle between 329° and 351° with respect to North[11].

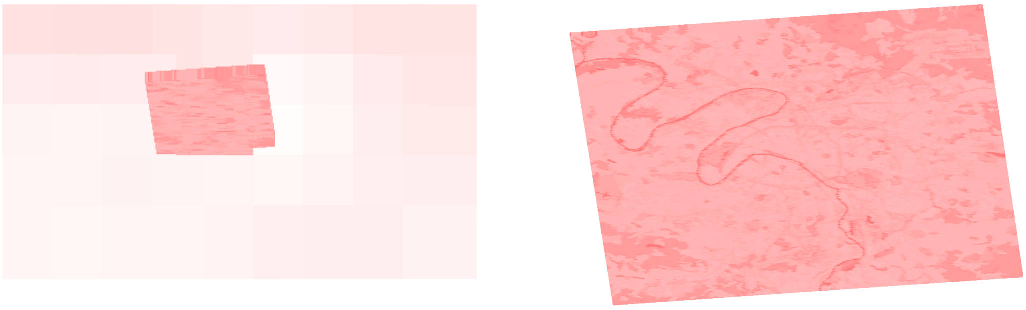

(a) Île de France (b) Zoom over Paris

Figure 6: Map of wind speed over Île-de-France for June 2017. Source: Copernicus Climate and ERA5

We also examine the measure concentration of O_3 in air pollution control stations that have been classified as being Rural (located out of the urban plume major direction), in order to calibrate the constant ratio of the Leighton relationship. Meaning that they are not influenced by human activities such as road traffic emissions or industrial emissions. This allows us to assess the background level of O_3 in Île-de-France. Which gives us the value that the $\frac{J_1}{k_3}$ has to take in order to reproduce it in absence of NO_x emissions (e.g under null concentration of NO and NO_2). The analysis reveal that the background concentrations of O_3 in Île-de-France is around $45\mu g.m^{-3}$. Therefore, we calibrate the constant ratio of the Leighton relation to 5.5384 which corresponds to the ratio under which the concentration of O_3 is $42.7\mu g.m^{-3}$.[12]

4.5 Inputs for costs evaluations

The marginal cost of CO_2 (in €$.T^{-1}$) used in this study is 100 and the marginal costs of fuel (in €$.kg^{-1}$) is 2.516 which represents a price of 2€$.L^{-1}$

[11] More parameter values are available in Annexe 1

[12] See Appendix 3 for graphic informations

Our population and monetization model focuses solely on assessing the economic costs of mortality due to air pollution exposure, with morbidity being the most severe consequence, backed by robust evidence. The population exposure marginal costs functions are derived from the Environmental European Agency (EEA) methodology[13] used by de Bruyne and de Vries, (2020). This methodology can be divided in two steps.

First, in order to calculate the health risks associated with air pollution, one may utilize concentration-response functions. These functions, established by epidemiological literature, illustrate the correlation between the concentration of an air pollutant to which a population is exposed and the associated risk of a health outcome (WHO, 2013).

Subsequently, once the health outcomes related to population exposure to air pollution are estimated, their economic value can be determined through appropriate monetization methods, as outlined by **DEBR** (**DEBR**). This comprehensive methodology enables us to quantify the economic costs associated with air pollution-related mortality impacts.

Table 2.3 presents the value of those population exposure costs function for each pollutants. They represent the costs of being exposed during one hour to a concentration C_k of pollutant k.[14]

Table 3: Population exposure marginal costs functions for O_3, $PM_{2.5}$, and NO_2

Pollutant	$c(C_k)$ (in €/ $\mu g.m^{-3}$ / h)
O_3	$[\frac{exp(3.31\times10^{-8}\times C_k)-1}{exp(3.31\times10^{-8}\times C_k)} - 0.6322] \times 7979.4$
$PM_{2.5}$	$[\frac{exp(7.08\times10^{-7}\times C_k)-1}{exp(7.08\times10^{-7}\times C_k)}] \times 7979.4$
NO_2	$[\frac{exp(8.68\times10^{-8}\times C_k)-1}{exp(8.68\times10^{-8}\times C_k)}] \times 7979.4$

[13]https://www.eea.europa.eu/publications/assessing-the-risks-to-health

[14]More information about their computations are available in Appendix 4

It is noteworthy that the function associated with O_3 consistently produces negative values: if we increase traffic, NO_x is increasing and O_3 decreasing. This is a consequence of the local emissions of NO_x from road traffic, resulting in a local depletion of O_3. Therefore, the reduction in local O_3 concentrations due to road traffic is perceived as a positive local outcome rather than a drawback[15]. Nevetheless, it is also known that NO_x emission reductions (resp. increases) will help to reduce (resp. increase) ozone concentrations downwind due to chemistry and NO_x reactions with $VOCs$ (Volatile Organic Compounds).

5 Results: Exposure evaluation of Franciliens to the road traffic air pollution

This section of the chapter describes the findings of our research for Île-de-France, which will be used as a baseline to compare the efficiency of the policy under examination. We will show three sets of results. First, we will go over the results of the road traffic simulation. Second, we will discuss the estimated emissions of air pollutant generated by road traffic. Finally, we will provide the METRO-TRACE outputs, which show the population exposure costs to road traffic air pollution.

5.1 Traffic simulations

The traffic simulation results are summarized in Table 2.4. Based on our simulation during a typical morning period (between 3 and 10 a.m), over 2.5 million trips are made using cars in Île-de-France, constituting 30% of the total trips which is lower than estimated in the EGT (Enquête Global Transport) for Île-de-France with a value of 37.8%. These trips typically cover an average distance of 12.6 km and have an average duration of 20 minutes and 33 seconds which is comparable with the figure estimate in the EGT for Île-de-France coming at 22 minutes 40 seconds. Given the average speed of 38.8 $km.h^{-1}$, it can be inferred that a majority of these trips occur on urban roads with speed limitations of 50 $km.h^{-1}$. Moreover, Durrmeyer and Martinez (2022) has estimated using a microeconomics founded transportation model that average trip distance in Île-de-France is about 12.92 km with an average duration of 34 minutes

[15]Refer to Annex 1 for further insights on the photostationary steady state.

45 seconds. He also estimated that the share of trips by car is about 35%.

Table 4: Summary of METROPOLIS2 traffic simulations over Île-de-France from 3 a.m to 10 a.m

Index name	**Index simulated value**	**Index definition**
Number of trip	2,580,120	Total number of trips made by car
Share of car trip (%)	30	Share of trips made by car among all trips
Trip duration	20min 34sec	Mean travel time
Trip distance (km)	12.609	Mean travel distance
Mean speed ($km.h^{-1}$)	38.8	Mean travel speed
Total vehicle kilometer ($km \times 10^6$)	32.5	Total kilometers traveled
Total value of time (€$\times 10^6$)	41.6	Sum of the generalized travel costs of each agents

Figure 2.7 illustrates the hourly distribution of activities on the network, represented by the number of vehicle kilometers. These activities exhibit a strong correlation with emissions. The graph indicates that the majority of journeys take place between 6 and 10 a.m., with the network reaching its peak activity levels between 8 and 9 a.m.

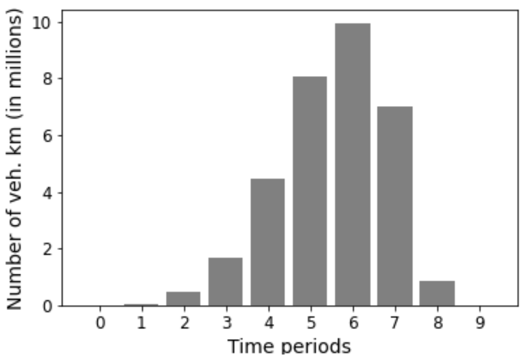

Figure 7: Activity per hour (in vehicle kilometer) computed from METROPOLIS2 on Île-de-France

These first results highlight the fact that car commuting in Île-de-France is not to predominante. Moreover, since drivers seems to drive in majority on small road with speed limits lower than 70 $km.h^{-1}$ at a first stage it is straightforward to think that speed limitations policies in Île-de-France should not have a very large effect.

5.2 Emission simulations

The integration of METROPOLIS2 traffic simulations with the EMISENS model enables the computation of air pollutant emissions for CO, CO_2, NO_x, and $PM_{2.5}$. These emissions are detailed in Table 2.5.

Table 5: Total air pollutant traffic emissions of CO, CO_2, NO_x, and $PM_{2.5}$, as well as Fuel Consumption (FC) computed over Île-de-France

For morning hours (from 3 a.m. to 10 a.m.)				
Pollutant	**Total (kg)**	**Per driver (g)**	**Per inhabitant (g)**	**Per kilometer (g)**
CO	18,966	9.06	1.55	0.58
$PM_{2.5}$	901	0.43	0.07	0.03
NO_x	11,110	5.3	0.91	0.34
CO_2	5,705,257	2,720.91	467.26	175.37
FC	1,797,314	0.86	0.15	0.06
Per year (All days)				
Pollutant	**Total (T)**	**Per driver (kg)**	**Per inhabitant (kg)**	
CO	17,307	8.25	1.42	
$PM_{2.5}$	823	0.39	0.07	
NO_x	10,138	4.83	0.83	
CO_2	5,206,047	2,482.83	426.38	
FC	1,640,049	0.78	0.13	

It is observed that each driver emits approximately 2.5 T of CO_2 annually. Additionally, each driver contributes 4.8 kg of NO_x per year, a value slightly lower than the 8 $kg/driver/year$ estimate for Strasbourg by Ho, Clappier, and Blond (2014). The variation is attributed to the substantial evolution in the vehicle fleet between the two studies, notably a decrease in diesel cars. Furthermore, each driver releases 8.3 kg of CO and 0.4 kg of $PM_{2.5}$ annually. It is noteworthy that these latter two values are notably higher compared to our earlier estimates in the study conducted on La Réunion. Yin et al. (2024) estimate that the road traffic was responsible of the emissions of 31,000 kg of NO_x, 234 kg of $PM_{2.5}$ per day in Île-de-France. Interestingly, the results for NO_x are three times larger than our estimates for morning. Therefore, if we consider 2.5 peaks per days those values become much more similar. However, our estimates for $PM_{2.5}$ are much higher than their estimations, which can be explained by the absence of the non-exhaust emissions in their estimations.

Figures 2.8 illustrate the emission patterns for our four types of pollutants. Typically, the temporal profile of emissions exhibits a strong correlation with the activity profile, such as the number of vehicle kilometers. Notably, we observe that the majority of emissions occur between 6 a.m. and 10 a.m., revealing a distinct pattern associated with the morning peak commute.

Given the significant influence of fleet composition, congestion, and other network factors on emissions, it is crucial to emphasize that these results are challenging to compare directly with other statistics available in the literature.

5.3 Road-traffic related air pollution simulation

In order, to examine our simulated concentration, we compare it to the one measure by AirParif in their air quality measurement station that they have designated as being influenced by road traffic for NO_2, NO, and $PM_{2.5}$. We present in this section only stations for which we have the measure of the three pollutants others stations are available in Appendix.

Figure 2.9 compares the findings of our air quality model at several locations to measured quantities of NO_2, NO, and $PM_{2.5}$. The observed concentrations were adjusted to account for causes other than road traffic. The mean concentration measured between 12 p.m. and 3 a.m. was removed. Our results seems to be in line with the observed concentrations for stations in Saint Denis and Gonesse. The fit is less evident for the Melun station, while our model seems to clearly under estimate the observed concentrations in Melun. Interestingly, it seems that our model estimates a bit higher concentrations of $PM_{2.5}$ while comparing with the observations on the field compare to what is obtained for NO and NO_2.

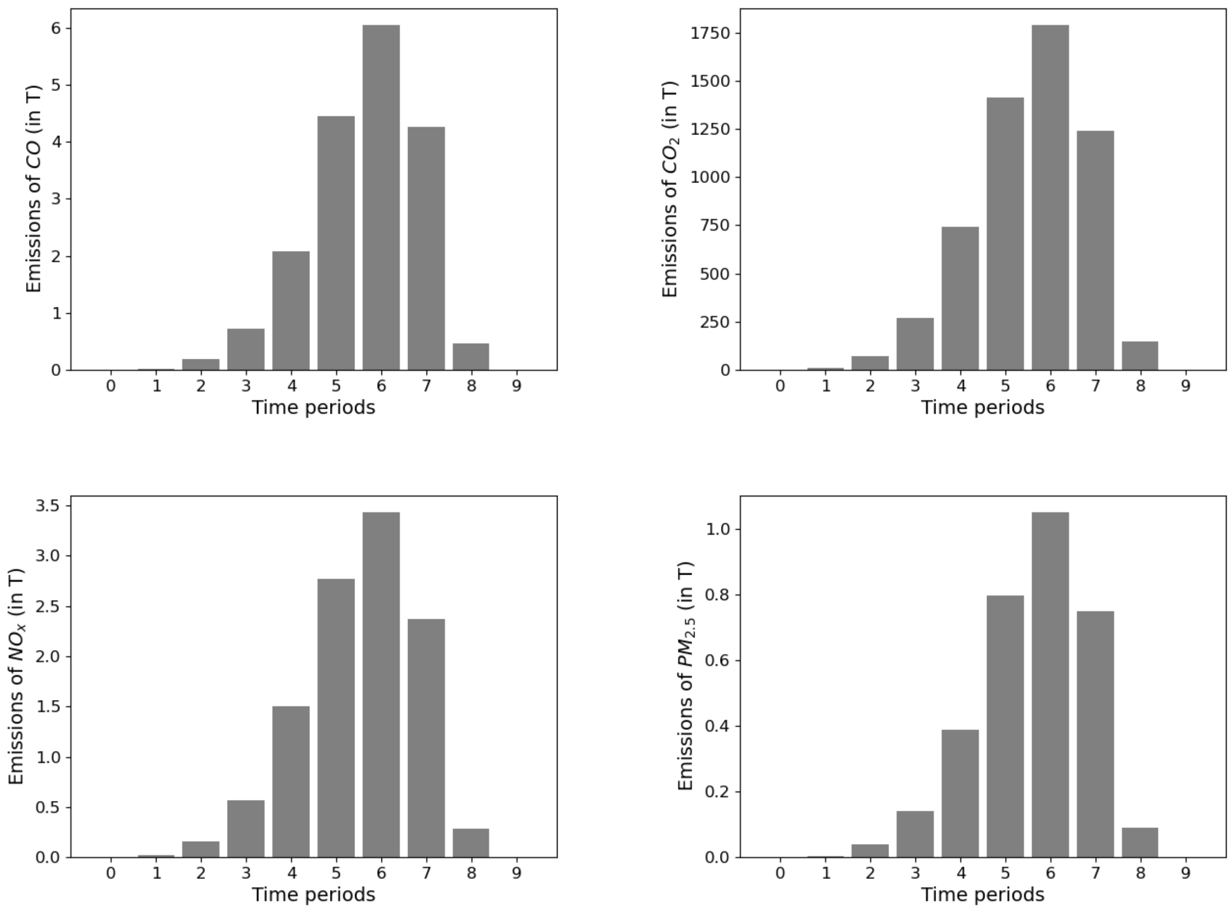

Figure 8: Total traffic air pollutant emissions of CO, CO_2, NO_x, and $PM_{2.5}$ per hour during the morning hours (in tons)

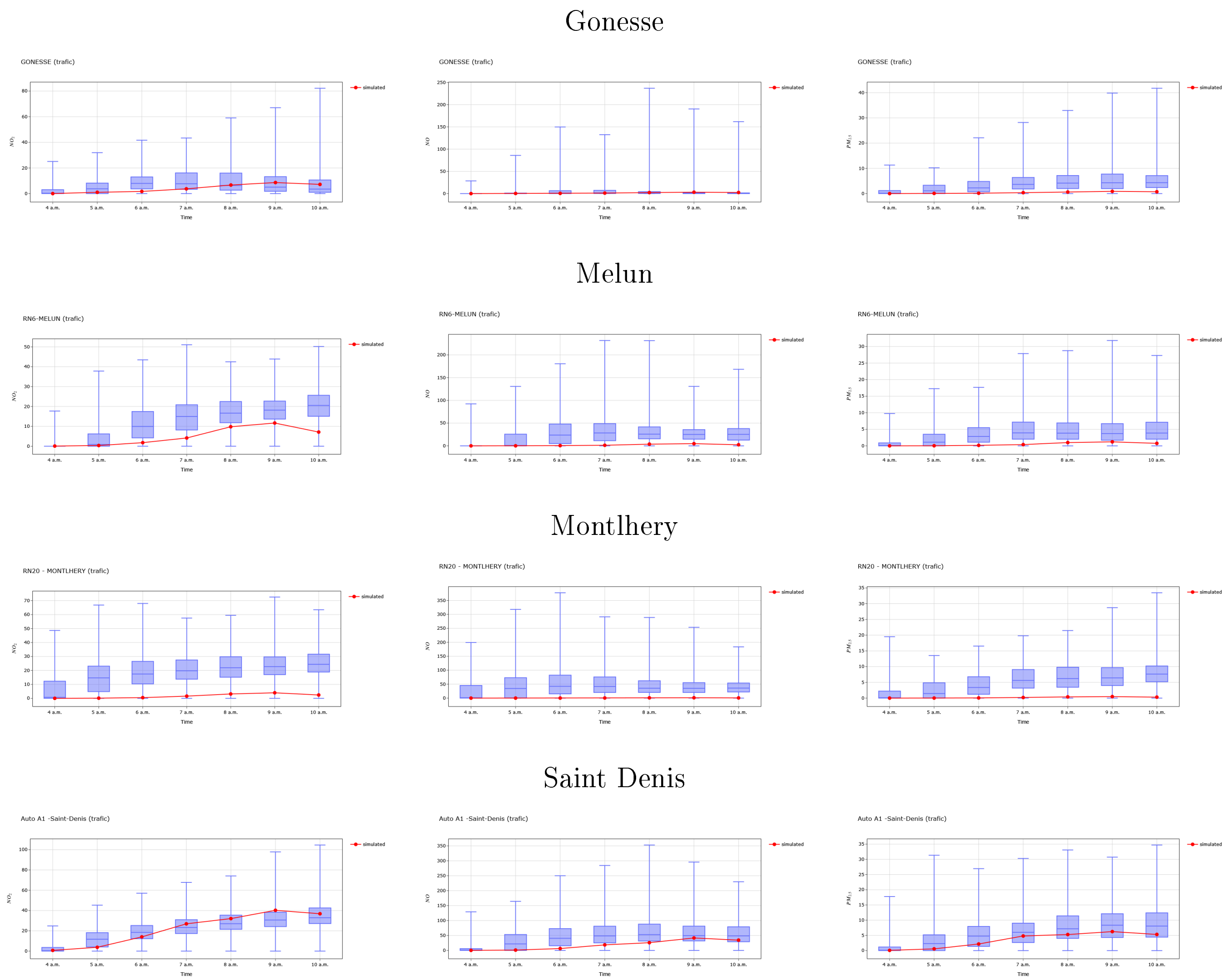

Figure 9: Observed concentrations of NO_2, NO, and $PM_{2.5}$ in air pollution station in Île-de-France during 2021 compared with simulated values. Source: LCSQA and AirParif

This comparison demonstrates that even in certain locations, our results slighly differ from what is observed and measured. Our model can still in average accurately predict concentrations of air pollutants caused by road traffic.

5.4 Exposure evaluations

Table 6 delineates the expenditures linked to the public's exposure to NO_2, O_3, and $PM_{2.5}$, along with the environmental costs associated with CO_2. It is important to underscore that these costs can be categorized as follows: CO_2, NO_2, and $PM_{2.5}$ contribute to 26%, 36%, and 37% of the overall costs of road traffic, respectively. In contrast, O_3 alleviates these costs by -29%. Consequently, it is pivotal to acknowledge that a significant portion of the costs attributed to NO_2 is counteracted by the reduction associated with O_3 destruction, underscoring the importance of considering the chemical process of O_3 creation in conducting this form of cost-benefit analysis. Furthermore, a sole emphasis on the cost analysis of CO_2 may lead to either an overestimation or underestimation of the externalities' benefits or costs arising from road traffic.

Upon a significant comparison of our findings with the reference values provided by the French government[16], it becomes evident that our estimated value of 0.047 €$.km^{-1}$ falls within the recommended range for project evaluation in very dense urban areas (0.116 €$.km^{-1}$) and dense urban areas (0.032 €$.km^{-1}$). Given that our study area encompasses a mix of both very dense and dense urban areas, the positioning of our estimate between these two values underscores the robustness of our approach.

Furthermore, our results can be compared to the cost benchmarks defined by the European Commission for France (Friedrich and Quinet, 2011). The EC suggests utilizing values of 27.2 €$/kgNO_x$ and a range between 131 and 407 €$/kgPM_{2.5}$ depending on characteristics of the studied area for the cost analysis of transportation projects. Notice that our estimates are quite larger than those values.

As reported by **DEBR** (**DEBR**), the annual cost of population exposure to PM_{10}, $PM_{2.5}$, NO_2, and O_3 in Paris is estimated at 1,602€/inhabitant. Notably, our results indicate a relatively lower cost compared to findings by Vlachokostas et al. (2012) and Martinez et al. (2018), who reported values of \$4,500 and \$3,601 per inhabitant, respectively. It is crucial to note that

[16] https://www.ecologie.gouv.fr/sites/default/files/V.2.pdf

Table 6: Total air pollutant traffic exposure costs to CO_2, NO_2, O_3, and $PM_{2.5}$ computed over Île-de-France

For morning hours (from 3 a.m. to 10 a.m.)					
Pollutant	**Total (k€)**	**Per driver (€)**	**Per inhabitant (€)**	**Per kilometer (€)**	**Per emission (€.kg^{-1})**
NO_2	784.8	0.374	0.067	0.024	70.64
$PM_{2.5}$	810.2	0.386	0.069	0.025	898.78
O_3	-638.6	-0.305	-0.054	-0.02	-
CO_2	570.5	0.272	0.049	0.018	0.1
Total	1527	0.728	0.13	0.047	-
Per years (All days)					
Pollutant	**Total (M€)**	**Per driver (€)**	**Per inhabitant (€)**		
NO_2	716.1	341.52	60.96		
$PM_{2.5}$	739.3	352.60	62.93		
O_3	-582.7	-277.9	-49.6		
CO_2	520.6	248.28	44.32		
Total	1393.3	664.50	118.61		

these costs include the population exposure to pollutants from all sources. Our estimations for Île-de-France imply a cost of around 118.6 €per inhabitant. However, this number is exclusively linked to road traffic; other sources are ignored.

Several factors contribute to the observed discrepancy in values. One notable distinction is that many studies do not explicitly consider population exposure. Our study, however, meticulously accounts for the spatial and temporal distribution of both population and concentrations. In contrast, in de Bruyne and de Vries (2020), for instance, residents are assumed to be exposed to average concentrations observed in the studied area, potentially leading to significant differences.

Additionally, it is crucial to note that our models do not incorporate road traffic associated with public transportation. Furthermore, while population exposure is predominantly influenced by the spatial distribution of population and roads, variations in fleet composition, traffic flows, and congestion significantly impact pollutant emissions. Therefore, comparing population exposure to vehicle traffic pollution statistics across different nations, regions, or municipalities poses a considerable challenge.

6 Results: Evaluation of speed limitations policy

This section presents the outcomes of assessing the effectiveness of speed limitation policies on high-pollution days in Île-de-France, i.e. reducing the speed of vehicle by 20 $km.h^{-1}$ with a minimum of 70 $km.h^{-1}$. To evaluate this policy, we simulate two distinct scenarios. The first scenario, named "without mode choice" is simulated without allowing agents to alter their mode of transportation. This reflects the low frequency of such speed limitation policies, which are often disclosed only 48 hours before they take effect, leaving drivers little time to adapt their behavior. However, we also simulate an alternate scenario, labeled "with mode choice" where agents have the flexibility to modify their mode of transportation. This scenario aims to assess the potential long-term impact of the policy if implemented continuously.

6.1 Traffic simulations

Table 2.7 presents the results of our dynamic traffic model uder speed limit restrictions for both scenarios. Significant differences are seen between the "without mode choice" scenario and the baseline. Following policy implementation, trip duration increases by 9%, trip distance by 5%, and average speed decreases by approximately 9%. This suggests that agents change their paths in response to the policy. In the "with mode choice" scenario, the average trip duration increases by 1.5%. However, trip distance drops by 3% which moderate this reduction leading to a change of the average speed of somewhat more than 9%.

As anticipated, this policy has an effect on the average speed at which vehicles travel due to the increased travel time. However, it is important to observe that both scenarios result in the same drop in average speed. Nevertheless, the average trip distance decreases in the "with mode choice" scenario which may implies that both scenarios might result in different outcomes at the end.

Table 7: Summary of METROPOLIS2 traffic simulations computed over Île-de-France from 3 a.m to 10 a.m, while adding restricting the speed limitations by 20 $km.h^{-1}$ with a minimum of 70 $km.h^{-1}$, while allowing or not for modal changes in the model

Statistic	**Without mode choice**		**With mode choice**	
	Values	**Difference (%)**	**Values**	**Difference (%)**
Number of trip by car	2,580,120	0	2,557,850	-0.9
Trip duration	22min 21sec	+8.7	20min 52sec	+1.5
Trip distance (km)	13.19	+4.6	12.246	-2.9
Mean speed ($km.h^{-1}$)	35.42	-8.7	35.2	-9.3
Total vehicle kilometer ($km \times 10^6$)	34	+4.6	31.3	-2.9
Total value of time (€$\times 10^6$)	42.2	+1.4	41.8	+0.5

6.2 Emission simulations

Table 2.8 presents the findings from EMISENS for both scenarios, highlighting a noteworthy reduction in the overall emissions of CO, CO_2, NO_x, and $PM_{2.5}$, as well as the Fuel consumption (FC).

In the scenario without mode choice, there is no evidence that pollutant emissions are affected by the policy. Conversely, the outcomes for the scenario with mode choice differ. Emission of CO_2 as well as FC are reduced by the implementation of the policy by 5%, while CO and NO_x exhibits a bit higher reduction coming at 8%. Interestingly, this policy as no effect on the $PM_{2.5}$ emissions which may be due to the fact that $PM_{2.5}$ are the only pollutant that is both resulting for exhaust and non-exhaust sources.

6.3 Exposure evaluations

Table 2.9 illustrates the population exposure costs and environmental costs associated with our two scenarios. Notably, as CO_2 costs exhibit a linear relationship with emissions, a corresponding decrease is observed. In the "without mode choice" scenario since there is no effect on the emission of pollutant, the exists nearly no effect of the policy on the population exposure costs

Table 8: Total air pollutant traffic emissions of CO, CO_2, NO_x, and $PM_{2.5}$ computed over Île-de-France from 3 to 10 a.m, while adding restricting the speed limitations by 20 $km.h^{-1}$ with a minimum of 70 $km.h^{-1}$, while allowing or not for modal changes in the model

Without mode choice				
Pollutant	**Total** (kg)	**Per driver** (g)	**Per inhabitants** (g)	**Per kilometer** (g)
CO_2	5,688,978 (-0.29%)	2,813.51 (+3.40%)	465.93 (-0.29%)	175.83 (+0.25%)
CO	18,927 (-0.21%)	9.36 (+3.32%)	1.55 (-0.21%)	0.58 (+0.86%)
NO_x	11,070 (-0.36%)	5.47 (+3.3%)	0.91 (-0.37%)	0.34 (+0.63)
$PM_{2.5}$	895 (-0.7%)	0.44 (+2.99%)	0.07 (-0.69%)	0.03 (-0.11)
FC	1,792,185 (-0.29%)	886.33 (+3.4%)	146.78 (-0.29%)	55.39 (+0.27%)
With mode choice				
Pollutant	**Total** (kg)	**Per driver** (g)	**Per inhabitants** (g)	**Per kilometer** (g)
CO_2	5,416,599 (-5.06%)	2,607.41 (-4.17%)	443.62 (-5.06%)	172.93 (-1.41%)
CO	17,475 (-7.86%)	8.41 (-7.15%)	1.43 (-7.66%)	0.56 (-3.81%)
NO_x	10,155 (-8.6%)	4.89 (-7.81%)	0.83 (-8.61%)	0.32 (-4.65%)
$PM_{2.5}$	907 (+0.66%)	0.44 (+1.6%)	0.07 (+0.66%)	0.03 (+4.6%)
FC	1,706,378 (-5.06%)	821.4 (-4.17%)	139.75 (-5.06%)	54.48 (-1.38%)

as well as on the environmental cost.

However, in the "with mode choice" scenario, we estimate a decrease of 5% of the CO_2 environmental costs. We also estimate that the policy should reduce NO_2 exposure costs by 4%, 2% for O_3 as well as for $PM_{2.5}$. Finally, resulting in a reduction of 4.1% of the total exposure costs.

The results emphasize the importance of employing a comprehensive model chain, such as the one utilized in this chapter, when assessing road traffic policies and their associated costs. Firstly, it is evident that in the "with mode choice" scenario, the costs per emission undergo significant alterations compared to the baseline scenario. Consequently, relying solely on marginal costs per emission quantity can result in both overestimating and underestimating the impact of the policy on NO_2 and $PM_{2.5}$ exposure costs. Additionally, the use of marginal costs per emitted quantities fails to account for population exposure to O_3. Moreover, in the "with mode choice" scenario, the cost per kilometer for population exposure to $PM_{2.5}$ is influenced by the policy, indicating that utilizing marginal costs per kilometer to evaluate road traffic policies is also unsuitable.[17]. Moreover, as it is shown in Le Frioux, de Palma, and Blond (2023), it is possible to have at the same time a reduction of the emission and an increase of the population exposure costs. Therefore, in that specific case, using marginal costs per emitted quantities will lead to incorrect estimation of the effect of the policy.

Our findings emphasize the critical need of including population exposure in the evaluation of pollution reduction policies. The policy effectively decreases emissions of CO, CO_2, NO_x, and $PM_{2.5}$, resulting in an overall drop in pollution costs. However, a detailed study indicates that, despite reduced emission amounts, $PM_{2.5}$ increases. This emphasizes the need for policymakers to recognize that efforts to reduce particular pollutants may accidentally increase others, possibly leading to increased population exposure costs. As a result, policymakers must carefully consider the trade-offs associated with various pollution releases. This requires a comprehensive approach that considers both emission reduction and population exposure reduction

[17]More details about computation with the other methodologies are available in Appendix

Table 9: Total air pollutant traffic costs for CO_2, NO_2, O_3, and $PM_{2.5}$ computed over Île-de-France from 3 to 10 a.m, while adding restricting the speed limitations by 20 $km.h^{-1}$ with a minimum of 70 $km.h^{-1}$, while allowing or not for modal changes in the model

			Without mode choice		
Pollutant	**Total (k€)**	**Per driver (€)**	**Per inhabitants (€)**	**Per kilometer (€)**	**Per emissions** (€.kg^{-1})
CO_2	569 (-0.29%)	0.281 (+3.4%)	0.048 (-0.29%)	0.018 (+0.27%)	0.1 (0.0%)
NO_2	781 (-0.44%)	0.386 (+3.25%)	0.067 (-0.44%)	0.024 (+0.11%)	70.58 (-0.08%)
O_3	-639 (+0.09%)	-0.316 (+3.8%)	-0.054 (+0.09%)	-0.02 (+0.65%)	- -
$PM_{2.5}$	798 (-1.51%)	0.395 (+2.14%)	0.068 (-1.51%)	0.025 (-0.96%)	891.39 (-0.82%)
Total	1509 (-1.17%)	0.746 (+2.49%)	0.128 (-1.17%)	0.047 (-0.62%)	- -
			With mode choice		
Pollutant	**Total (k€)**	**Per driver (€)**	**Per inhabitants (€)**	**Per kilometer (€)**	**Per emission (€)**
CO_2	542 (-5.06%)	0.261 (-4.17%)	0.046 (-5.06%)	0.017 (-1.39%)	0.1 (0.0%)
NO_2	751 (-4.29%)	0.362 (-3.4%)	0.064 (-4.29%)	0.024 (-0.59%)	73.96 (+4.71%)
O_3	-626 (-1.92%)	-0.301 (-1%)	-0.053 (-1.92%)	-0.02 (+1.87%)	- -
$PM_{2.5}$	797 (-1.58%)	0.384 (-0.66%)	0.068 (-1.58%)	0.025 (+2.22%)	878.82 (-2.22%)
Total	1464 (-4.13%)	0.705 (-3.24%)	0.125 (-4.13%)	0.047 (-0.43%)	- -

objectives. Policies that follow this principle can provide the most significant benefits to public health and the environment.

6.3.1 Conclusions of the evaluation of the policy

Table 2.10 summarize the costs-benefits analysis of the policy for both scenarios. Those results suggest that implementing the policy as it is done nowadays only for some days without giving time to agent in order to adapt leads to increase substantially the travel time costs of agent with almost no effect on population exposure costs underlying the inefficiency of the policy. However, interestingly when agents have time to adapt to the policy (e.g. if the policy is implemented in the long run), the travel time costs of agents are slightly increased but largely compensated by the savings on fuel consumption, environmental, and population exposure costs.

Table 10: Summary of the evaluation of the policy

Without mode choice		
	Value (in k€)	**Diff. (in k€)**
Travel time costs	42,224	+613
Fuel consumption costs	4,217	-12
Environmental costs	569	-2
Population exposure costs	940	-16
Total	47,950	+583
With mode choice		
	Value (in k€)	**Diff. (in k€)**
Travel time costs	41,796	+185
Fuel consumption costs	4,015	-214
Environmental costs	542	-34
Population exposure costs	922	-13
Total	47,248	-76

Therefore, we can conclude that this policy if not anticipated is inefficient to reduce population exposure costs to road traffic pollution in the short run and very detrimental for population well-being meaning that the gain due to the reduction of the population exposure cost, the environmental costs and the fuel consumption reduction does not offset the lost in welfare. While in the long run the policy could have some more significant positive impact on environmental, population exposure costs, and fuel consumption. Nevertheless, when taking into account the welfare losses this gain is seems somewhat marginal. We can notice that those findings are in line with the estimates of Durrmeyer and Martinez (2022) which finds that generally reduction in local and global pollutants represents a small fraction of gain compared to welfare losses.

Therefore, in order to efficiently implement this policy policymarkers should give opportunity to agents to adapt to the policy. Therefore, this type of policy can not be used as an emergency approach without considering other additive measure such as increasing public transit frequencies and/or capacities, reducing the price of public transit fees, rising taxes on road transit.

Nevertheless, our analysis is not taking into account all the benefits that can be associated with such policies such as noise reduction and higher level of road traffic savety. Using Maibach et al. (2008) it is possible to estimates that speed limitations policies will raise the overall costs of car accident by 21,150€ in the "without mode choice" scenario and reduce it by 16,920€ in the "with mode choice"[18]. Concerning noise the estimations are more complex and necessitate a proper integrated chain of model for population exposure to road-traffic noises in order to take into account also for displacement effect, diffusion, as well as population exposure. According to Bühlmann and Egger (2017), speed limits restrictions can reduce noise by 1 to 5 dB close to the road depending on lot of influencing factors.

6.4 Decomposition of the policy

In this section, we delve into the impact of the policy by dissecting it into three distinct scenarios. This approach not only provides a nuanced understanding of the policy's effects but also allows us to address pivotal questions central to the French public debate on road traffic policies, such as contemplating the reduction of highway speed (e.g., lowering the speed from

[18]Those costs are computed using an average marginal costs of 0.0141 €.km^{-1}.

130 $km.h^{-1}$ to 110 $km.h^{-1}$)[19].

Table 2.11 summarizes the costs-benefits analysis of the policy if implemented in the long run.

Table 11: Summary of costs-benefits computed over Île-de-France from 3 a.m to 10 a.m when decomposing the effect of the policy

Reducing speed to 70 $km.h^{-1}$ for speed lower than 90 $km.h^{-1}$		
	Value (k€)	**Diff.**
Travel time costs	41,507	-104
Fuel consumption costs	4,204	-25
Environmental costs	567	-4
Population exposure costs	952	-4
Total	47,230	-137
Reducing speed by 20 $km.h^{-1}$ for speed from 90 to 110 $km.h^{-1}$		
	Value (k€)	**Diff.**
Travel time costs	42,100	+489
Fuel consumption costs	4,243	+14
Environmental costs	572	+1
Population exposure costs	948	-8
Total	47,863	+496
Reducing speed by 20 $km.h^{-1}$ for speed from 110 to 130 $km.h^{-1}$		
	Value (k€)	**Diff.**
Travel time costs	41,451	-160
Fuel consumption costs	4,213	-16
Environmental costs	958	+3
Population exposure costs	380	+2
Total	47,002	-177

It is interesting to note that the three alternative scenarios have essentially little influence on environmental or population exposure costs. This implies that lowering speed restrictions on roadways is not an effective way to combat air pollution. This suggests that lowering

[19] Note that all simulations in this section are made using mode choice.

speed restrictions may not be an effective method to decrease road traffic-related air pollution. Moreover, in the case of the reduction of speeds by 20 $km.h^{-1}$ at speeds ranging from 90 to 110 $km.h^{-1}$ considerable increases in agents' travel time costs and fuel consumption can be observed suggering that due to such policies agents may incur significant costs in the long run. As a result, such policies are ineffective to tackle air pollution issues. and can be costly for agents. Therefore such policies should not be regarded a feasible solution to air pollution problems in our particular setting.

7 Conclusions

We have developed an integrated chain of models to examine population exposure to air pollution resulting from car traffic. This comprehensive approach involves coupling a dynamic traffic simulation model, an emission model, an air quality model, and a population exposure model that incorporates cost evaluation. Time-discrete speed and flow distributions are harmonized with population motion data. The methodology estimates the cost of inhabitants' exposure to pollutants such as nitrogen dioxide (NO_2), Ozone (O_3), and particulate matter with a diameter lower than 2.5 µm ($PM_{2.5}$). Additionally, the cost of carbon dioxide (CO_2) is considered. Applying this chain to compute pollution costs in Île-de-France, we determined that the pollution costs for Francilian inhabitants amount to approximately 120€/year/inhabitant.

Our results demonstrate that implementing speed limit reductions for speeds exceeding 70 $km.h^{-1}$ effectively decreases emissions of CO, CO_2, and NO_x as well as fuel consumption (FC) from road traffic, only if agents anticipated and have time to adapt to the policy. Our results also suggests that lowering speed on highways or national road solely is not efficient to tackle road traffic air pollution issues and may increase the travel time and fuel consumption of drivers. Therefore, speed limit restrictions seems to not be a suitable tool in order to reduce overall air pollution.

While our model chain provides useful insights, there is potential for improvement, particularly in terms of increasing the range of population exposure based on socio-demographic variables and micro-environment. Furthermore, we forgot to include truck traffic and public transit in our research, which offer potential opportunities for improvement. Additional work is required to improve our model chain for convenience of use in future research and scenario testing. Furthermore, this model might be supplemented with additional models such as population noise exposure and car accident estimates to properly quantify the advantages and drawbacks of road traffic policy.

Our study underscores the critical importance of thoroughly evaluating the consequences outlined in this chapter before implementing road traffic policies. Furthermore, it highlights that not considering population exposure in such evaluations could lead to a misinterpretation of policy consequences.

Bibliography

References

[1] S.J. Arnold et al. "Introduction to the DAPPLE air pollution project". In: *Science of the Total Environment* 332.1-3 (2004), pp. 139–153.

[2] J. Bañeras et al. "Short-term exposure to air pollutants increases the risk of ST elevation myocardial infarction and of infarct-related ventricular arrhythmias and mortality". In: *International journal of cardiology* 250 (2018), pp. 35–42.

[3] Claus Bliefert and Robert Perraud. *Chimie de l'environnement: air, eau, sols, déchets (in French).* De Boeck Superieur, 2007.

[4] E. Bühlmann and S. Egger. "Assessing the noise reduction potential of speed limit 30 km/h". In: *Proceedings of the INTER-NOISE.* 2017.

[5] D. Carslaw and S. Beevers. "The efficacy of low emission zones in central London as a means of reducing nitrogen dioxide concentrations". In: *Transportation Research Part D: Transport and Environment* 7.1 (2002), pp. 49–64.

[6] G. Cesaroni et al. "Health benefits of traffic-related air pollution reduction in different socioeconomic groups: the effect of low-emission zoning in Rome". In: *Occupational and environmental medicine* 69.2 (2012), pp. 133–139.

[7] S. de Bruyne and J. de Vries. "Health costs of air pollution in European cities and the linkage with transport". In: *CE Delft* 190272 (2020).

[8] A. de Nazelle, D. Rodríguez, and D. Crawford-Brown. "The built environment and health: impacts of pedestrian-friendly designs on air pollution exposure". In: *Science of the Total Environment* 407.8 (2009), pp. 2525–2535.

[9] A. de Palma and F. Marchal. "Real cases applications of the fully dynamic METROPOLIS tool-box: an advocacy for large-scale mesoscopic transportation systems". In: *Networks and spatial economics* 2.4 (2002), pp. 347–369.

[10] S. Dhondt et al. "Health impact assessment of air pollution using a dynamic exposure profile: implications for exposure and health impact estimates". In: *Environmental impact assessment review* 36 (2012), pp. 42–51.

[11] D. Dias, O. Tchepel, and A. Antunes. “Integrated modelling approach for the evaluation of low emission zones”. In: *Journal of environmental management* 177 (2016), pp. 253–263.

[12] R.R. Dickerson, D. Stedman, and A. Delany. “Direct measurements of ozone and nitrogen dioxide photolysis rates in the troposphere”. In: *Journal of Geophysical Research: Oceans* 87.C7 (1982), pp. 4933–4946.

[13] E. Dons et al. “Using an activity-based framework to determine effects of a policy measure on population exposure to nitrogen dioxide”. In: *Transportation research record* 2233.1 (2011), pp. 72–79.

[14] I. Durrmeyer and N. Martinez. “The welfare consequences of urban traffic regulations”. In: (2022).

[15] H. Van Essen et al. *Handbook on the external costs of transport, version 2019.* 18.4 K83. 131. 2019.

[16] A. Etuman et al. “Addressing the issue of exposure to primary pollution in urban areas: Application to Greater Paris”. In: *Atmospheric environment* 239 (2020), p. 117661.

[17] D. Fang et al. “Mortality effects assessment of ambient PM2. 5 pollution in the 74 leading cities of China”. In: *Science of the Total Environment* 569 (2016), pp. 1545–1552.

[18] R. Friedrich and E. Quinet. “External costs of transport in Europe”. In: *A handbook of Transport Economics.* Edward Elgar Publishing, 2011.

[19] P. Garrett and E. Casimiro. “Short-term effect of fine particulate matter (PM2. 5) and ozone on daily mortality in Lisbon, Portugal”. In: *Environmental Science and Pollution Research* 18.9 (2011), pp. 1585–1592.

[20] S. Gurram, A. Stuart, and A. Pinjari. “Agent-based modeling to estimate exposures to urban air pollution from transportation: Exposure disparities and impacts of high-resolution data”. In: *Computers, Environment and Urban Systems* 75 (2019), pp. 22–34.

[21] P. Hanrahan. “The plume volume molar ratio method for determining NO2/NOx ratios in modeling—Part I: Methodology”. In: *Journal of the Air & Waste Management Association* 49.11 (1999), pp. 1324–1331.

[22] M. Hatzopoulou, J.Y. Hao, and E.J. Miller. “Simulating the impacts of household travel on greenhouse gas emissions, urban air quality, and population exposure”. In: *Transportation* 38.6 (2011), pp. 871–887.

[23] M. Hatzopoulou and E.J. Miller. “Linking an activity-based travel demand model with traffic emission and dispersion models: Transport’s contribution to air pollution in Toronto”. In: *Transportation Research Part D: Transport and Environment* 15.6 (2010), pp. 315–325.

[24] H. Hersbach et al. “ERA5 hourly data on pressure levels from 1940 to present, Tech. Rep.” In: (2023).

[25] B.Q. Ho, A. Clappier, and N. Blond. “Fast and optimized methodology to generate road traffic emission inventories and their uncertainties”. In: *CLEAN–Soil, Air, Water* 42.10 (2014), pp. 1344–1350.

[26] H. Hooyberghs et al. “Climate variables for cities in Europe from 2008 to 2017, version 1.0”. In: *Copernicus Climate Change Service (C3S) Climate Data Store (CDS)(Accessed 4 November 2022)* (2019).

[27] S. Hörl and M. Balac. “Synthetic population and travel demand for Paris and Île-de-France based on open and publicly available data”. In: *Transportation Research Part C: Emerging Technologies* 130 (2021), p. 103291.

[28] S. Host et al. “Implementation of various hypothetical low emission zone scenarios in Greater Paris: Assessment of fine-scale reduction in exposure and expected health benefits”. In: *Environmental research* 185 (2020), p. 109405.

[29] L. Javaudin and A. de Palma. “METROPOLIS2: A Multi-Modal Agent-Based Transport Simulator”. In: (2024).

[30] B. Kickhöfer and J. Kern. “Pricing local emission exposure of road traffic: An agent-based approach”. In: *Transportation Research Part D: Transport and Environment* 37 (2015), pp. 14–28.

[31] R. Le Frioux, A. de Palma, and N. Blond. *Assessing the Economic Costs of Road Traffic-Related Air Pollution in La Reunion*. Tech. rep. THEMA (THéorie Economique, Modélisation et Applications), Université de ..., 2023.

[32] W. Lefebvre et al. "Presentation and evaluation of an integrated model chain to respond to traffic-and health-related policy questions". In: *Environmental modelling & software* 40 (2013), pp. 160–170.

[33] P.A. Leighthon. *Photochemistry of air pollution*. New-York Acad., 1961.

[34] Y. Lu. "Beyond air pollution at home: Assessment of personal exposure to PM2. 5 using activity-based travel demand model and low-cost air sensor network data". In: *Environmental Research* 201 (2021), p. 111549.

[35] M. Maibach et al. "Handbook on estimation of external costs in the transport sector". In: *Ce Delft* 336 (2008).

[36] G.S. Martinez et al. "Health impacts and economic costs of air pollution in the metropolitan area of Skopje". In: *International journal of environmental research and public health* 15.4 (2018), p. 626.

[37] D.R. McCubbin and M.A. Delucchi. "The health effects of motor vehicle-related air pollution". In: *Handbook of Transport and the Environment*. Emerald Group Publishing Limited, 2003.

[38] A. Naqvi et al. "The spatial–temporal exposure to traffic-related Particulate Matter emissions". In: *Transportation Research Part D: Transport and Environment* 123 (2023), p. 103899.

[39] L. Ntziachristos et al. "COPERT: a European road transport emission inventory model". In: *Information technologies in environmental engineering*. Springer, 2009, pp. 491–504.

[40] A. Poulhès and L. Proulhac. "The Paris Region low emission zone, a benefit shared with residents outside the zone". In: *Transportation Research Part D: Transport and Environment* 98 (2021), p. 102977.

[41] E. Romberg et al. "N0-N02-Umwandlungsmodell fur die Anwendung bei Immissionsprognosen fur Kfz-abgase". In: *Gefahrstoffe-Reinhaltung Luft56* (1996), pp. 215–218.

[42] G.M. Rowangould. "A new approach for evaluating regional exposure to particulate matter emissions from motor vehicles". In: *Transportation Research Part D: Transport and Environment* 34 (2015), pp. 307–317.

[43] R. Smit, L. Ntziachristos, and P. Boulter. "Validation of road vehicle and traffic emission models–A review and meta-analysis". In: *Atmospheric environment* 44.25 (2010), pp. 2943–2953.

[44] J. Smith et al. "London hybrid exposure model: improving human exposure estimates to NO2 and PM2.5 in an urban setting". In: *Environmental science & technology* 50.21 (2016), pp. 11760–11768.

[45] O.G. Sutton. "The problem of diffusion in the lower atmosphere". In: *Quarterly Journal of the Royal Meteorological Society* 73.317-318 (1947), pp. 257–281.

[46] S. Vallamsundar et al. "A comprehensive modeling framework for transportation-induced population exposure assessment". In: *Transportation Research Part D: Transport and Environment* 46 (2016), pp. 94–113.

[47] W.S. Vickrey. "Congestion theory and transport investment". In: *The American Economic Review* 59.2 (1969), pp. 251–260.

[48] C. Vlachokostas et al. "Health effects and social costs of particulate and photochemical urban air pollution: a case study for Thessaloniki, Greece". In: *Air Quality, Atmosphere & Health* 5.3 (2012), pp. 325–334.

[49] H. Walton et al. "Understanding the health impacts of air pollution in London". In: *London: Kings College London, Transport for London and the Greater London Authority* 1.1 (2015), pp. 6–14.

[50] WHO. "Health Risks of Air Pollution in Europe—HRAPIE Project". In: *WHO: Geneva, Switzerland* (2013).

[51] A. Wiegand and N. Bofinger. "Review of empirical methods for the calculation of the diurnal NO2 photolysis rate coefficient". In: *Atmospheric Environment* 34.1 (2000), pp. 99–108.

[52] B. Yin et al. "Evaluation of low-traffic neighborhoods and scale effects: the Paris case study". In: *Transportation research record* 2678.1 (2024), pp. 88–101.

Appendixes

Correspondance table of Crit'air to fuel types and Euro standards

Correspondance table of Crit'air to fuel types and Euro standards

Vignette Crit'air	**Fuel types**	**EURO Standard**
Crit'air 1	Petrol	EURO 5 & EURO 6
Crit'air 2	Petrol	EURO 4
Crit'air 2	Diesel	EURO 5 & EURO 6
Crit'air 3	Petrol	EURO 2 & EURO 3
Crit'air 3	Diesel	EURO 4
Crit'air 4	Diesel	EURO 3
Crit'air 5	Diesel	EURO 2
Not classified	Petrol	EURO 1
Not classified	Diesel	EURO 1

Dispersion parameter values

Photostationary steady state

The photostationary steady-state equilibrium is established through reactions involving NO_2, NO, and O_3 as described in the following equations:

$$NO_2 + h.\nu \xrightarrow{J_1} NO + O$$
$$O + O_2 + M \xrightarrow{k_2} O_3 + M$$
$$NO + O_3 \xrightarrow{k_3} NO_2 + O_2$$

where NO_2 represents nitrogen dioxide, NO denotes nitric oxide, O signifies oxygen, O_2 represents dioxygen, O_3 stands for ozone, and M is a specified species acting as a contact partner. Additionally, $h.\nu$ refers to photons, J_1 represents the photolysis rates, and k_2 and k_3 are two chemical constants.

Dispersion parameter values

Parameter	Value
Standard deviation of lateral concentration ($\sigma_y^2(x)$)	$\frac{ax}{(1+bx)^e}$
Standard deviation of vertical concentration ($\sigma_z^2(x)$)	$\frac{dx}{(1+bx)^e}$
a	0.0787
b	0.0014
c	0.135
d	0.0745
e	0.465

These equations indicate that the concentrations of various species are in balance, determined by a photolysis rate coefficient J_1, along with two chemical rate constants , denoted as k_1 and k_2 (Bliefert and Perraud, 2007). The set of equations results in a "null cycle," where species concentrations remain constant. Due to the high reactivity of ozone and the abundance of dioxygen, ozone can be assumed to be in a steady state, leading to the photostationary steady state. The Leighton relationship can be derived from this equilibrium (Leighthon, 1961). Under the steady states assumptions the above system of equations can be sum up in this equivalence:

$$NO_2 + NO + O_3 \Leftrightarrow NO_2 + NO + O_3,$$

meaning that at the steady state there exists an equilibrium between NO_2, NO, and O_3 where:

$$\frac{d[NO_2]_{PSS}}{dt} = \frac{d[NO]_{PSS}}{dt} = \frac{d[O_3]_{PSS}}{dt} = 0,$$

where $[NO_2]_{PSS}, [NO]_{PSS}, [O_3]_{PSS}$ are respectively the concentrations of NO_2, NO, and O_3 at the photochemical steady state. Therefore, we can finally write:

$$\frac{d[NO_2]}{dt} = -J_1[NO_2]_{PSS} + k_3[O_3]_{PSS}[NO]_{PSS} = 0 \Rightarrow [O_3]_{PSS} = \frac{J_1[NO_2]_{PSS}}{k_3[NO]_{PSS}}.$$

Graphics of O_3 concentrations observed in Île-de-France

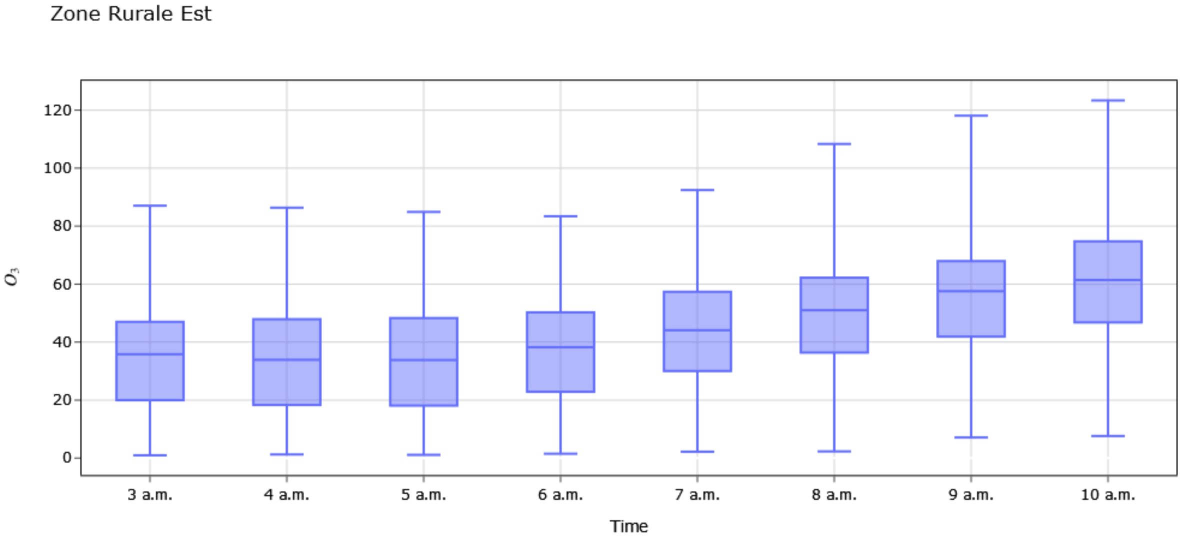

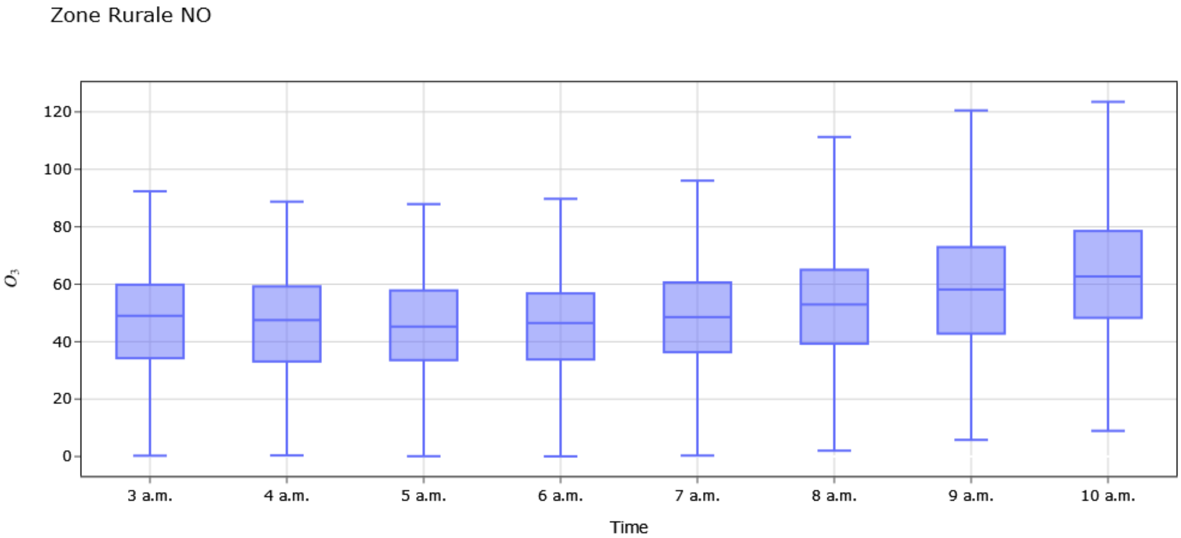

Zone Rurale Nord-Est

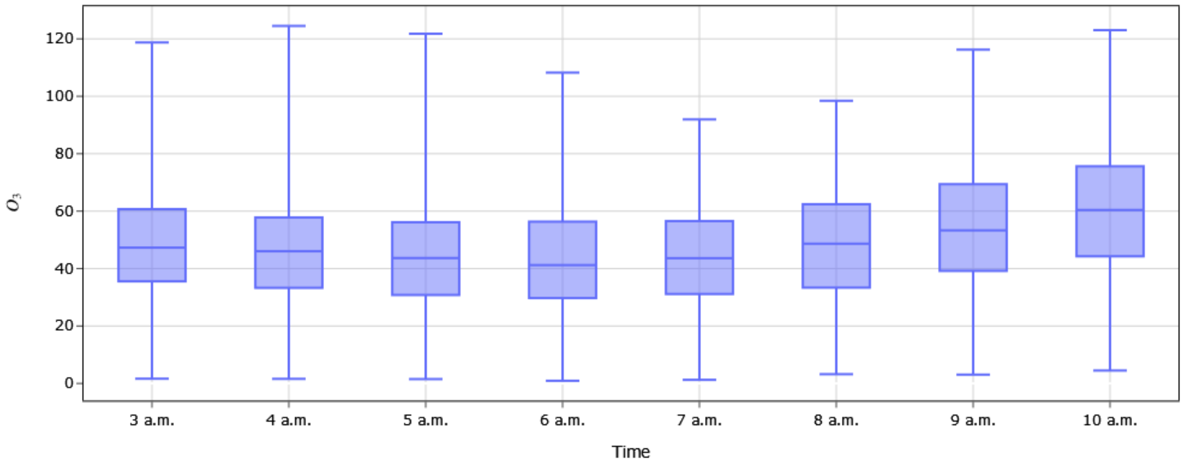

Zone Rurale SE

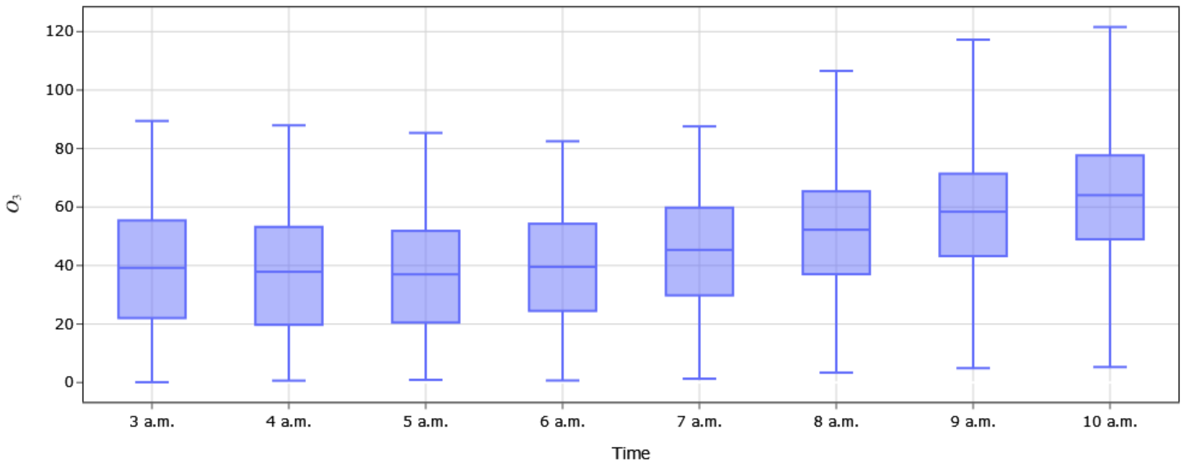

Zone Rurale SO

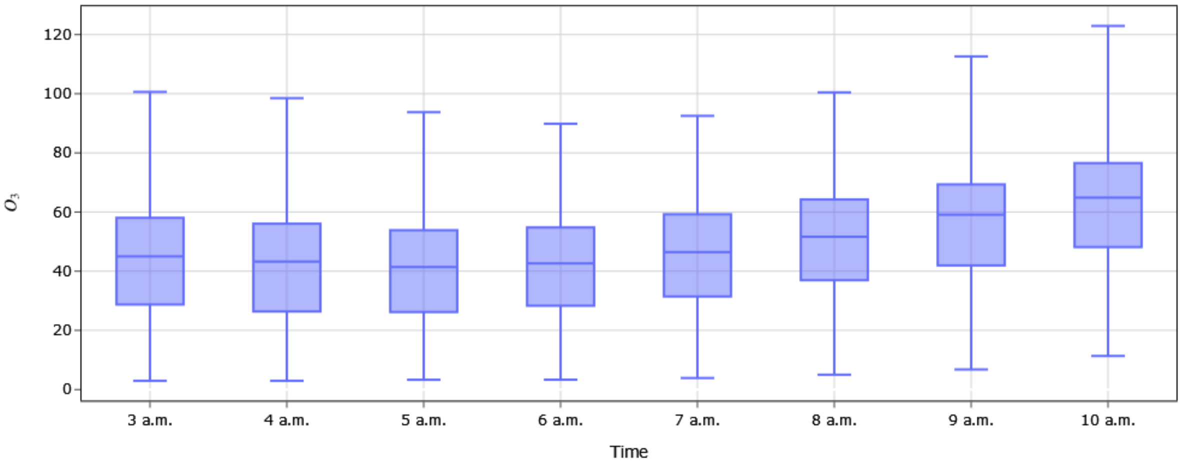

Zone rurale Sud

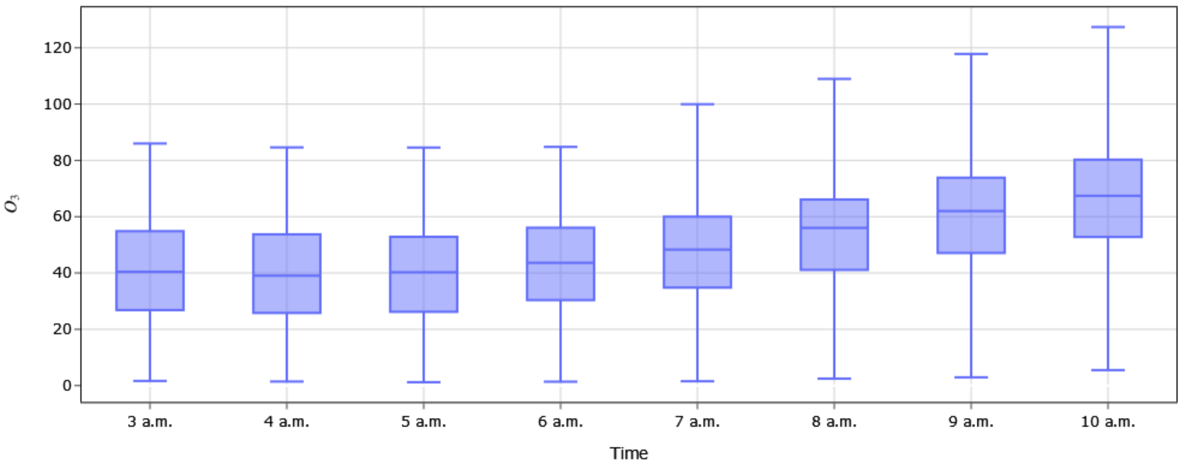

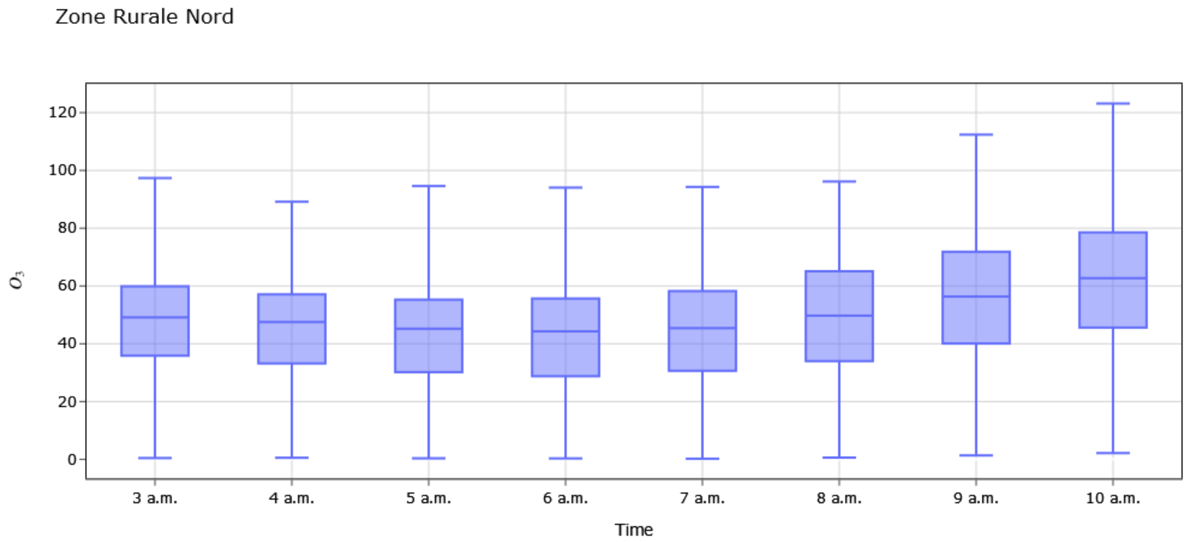

Observed concentrations of O_3 in rural air pollution station measure for the year 2021 in Île-de-France. Source: LCSQA and AirParif

Computation of the population exposure costs function

First, in order to assess the risk to health of air pollution it is mandatory to have values of the relative risks associated with the exposition to the air pollutant concentrations. They represent the increase of the health outcomes (here mortality) associated with a given increase in the air pollutant concentration. Those values have been retrieved from the WHO (2013) report.

However, those value are given for an increase of 10 $\mu g.m^{-3}$ of the annual concentrations. Therefore a value of 0.5 for example suggests that an increase of 10 $\mu g.m^{-3}$ of the annual concentration of a pollutant will raised the probability of dying by 50%.

Assuming linearity it is possible to compute those values for an increase of 1 $\mu g.m^{-3}$ of the hourly concentration using the following formula:

$$\beta_k^h = \frac{\beta_k^a}{10 \times 24 \times 365},$$

where β_k^h represents the impact of a 1 $\mu g.m^{-3}$ increase in the hourly concentration of pollutant k, while β_k^a denotes the effect of a 10 $\mu g.m^{-3}$ rise in the annual concentration of pollutant k. These specific values are detailed in this table.

Values of relative risks by type of pollutants. Source: WHO, 2013

Pollutant	β_k^a	β_k^h
O_3	0.0029	3.31×10^{-8}
$PM_{2.5}$	0.062	7.08×10^{-7}
NO_2	0.0076	8.68×10^{-8}

Hence, a β_k^h value of 3.31×10^{-8} for O_3 indicates that an increase of 1 $\mu g.m^{-3}$ of the hourly ozone concentration corresponds on average to a $3.31 \times 10^{-6}\%$ increase of the risk of mortality for population under consideration.

Therefore, those values can be used to compute the number of premature deaths linked to the hourly exposition to the concentration of pollutant k (in $\mu g.m^{-3}$) called Attributable Fraction ($AF(C_k)$) which represents the probability that the cause of a death can be attributable to the exposition to concentration level C_k of pollutant k:

$$AF(C_k) = \frac{exp(\beta_k^h \times C_k) - 1}{exp(\beta_k^h \times C_k)}$$

where, β_k^h is relative risk associated with the exposition to an hourly concentration of pollutant k and C_k is the hourly concentration of pollutant k (in $\mu g.m^{-3}$). For example an $AF(C_k)$ of 0.5 suggests that among people that are dying half of them are dying from the exposition to the concentration level C_k of pollutant k. Therefore, it is possible to estimate the probability for someone to die from the exposition to the pollutant using this formula:

$$Prob\ dying(C_k) = AF(C_k) \times mortality\ rate$$

where *mortality rate* is the natural mortality rate in the studied area. So, that if the *mortality rate* in the population is 50% and the AF is 0.5. The probability that someone die from this risk is 25%.

Finally, using the monetarization model it is possible to monetarize this probability. de Bruyne and de Vries (2020) propose the following approach:

$$c(C_k) = [AF(C_k) - AF(\overline{C_k})] \times \textit{mortality rate} \times AYL \times YOLL,$$

where $c(C_k)$ (in €.h^{-1}) is the costs function of being expose during one hour to a concentration C_k of pollutant k, $AF(C_k)$ is the attributable fraction of being expose during one hour to a concentration C_k of pollutant k, *mortality rate* is the natural mortality rate in the studied region (here 1%), AYL is the average number of year lost for someone dying from air pollution (here 10.4 years), and $YOLL$ is the price of a year of life lost (here 106,985€[20]).

Notice that $\overline{C_k}$ is the background concentration. It is only used to built the marginal costs function of O_3. Because O_3 is decreasing with road traffic activity it is important to considered it as a benefits and not a cost like for the others pollutants. Those Values of $\overline{C_k}$ for the different pollutants are given in the following table:

Values of the background concentration of pollutant

Pollutant	$\overline{C_k}$
O_3	42.7
$PM_{2.5}$	0
NO_2	0

[20]This value has been computed in order to take into account the purchasing power parity. It represents an average value of year of life lost of 70,000€.

Comparison of observed concentrations of NO_2, NO, and $PM_{2.5}$ against simulated concentrations

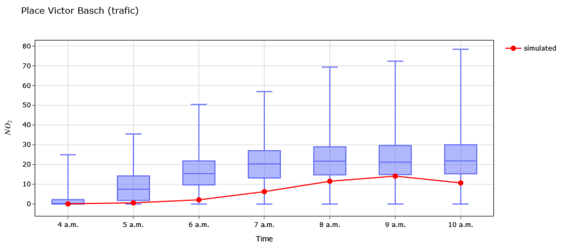

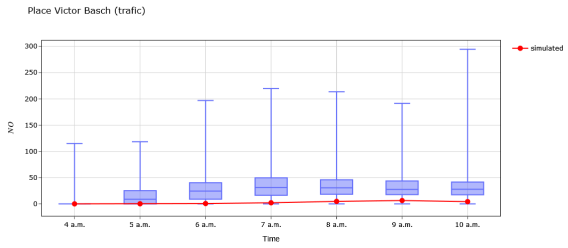

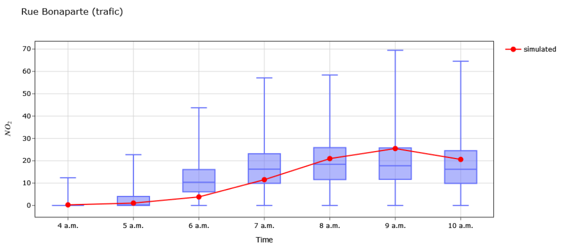

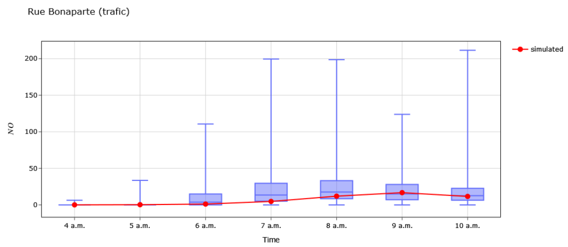

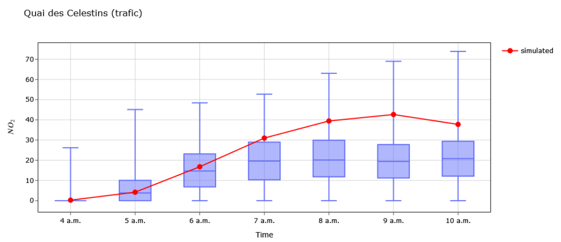

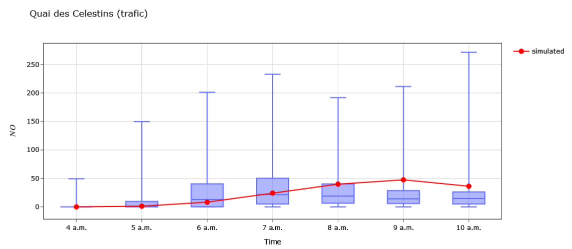

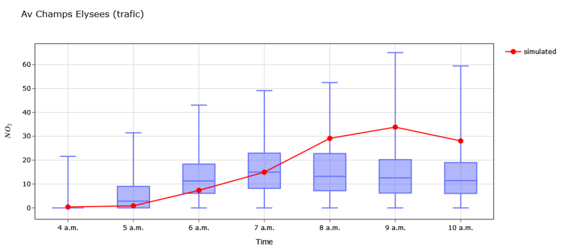

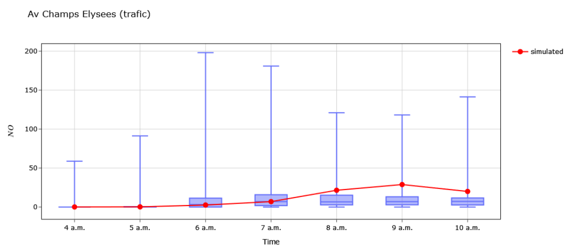

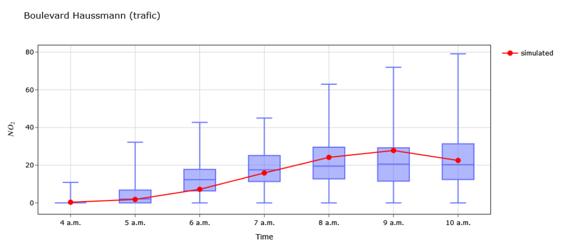

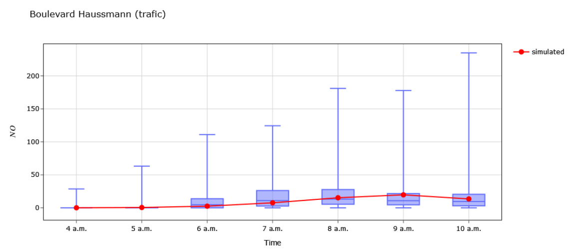

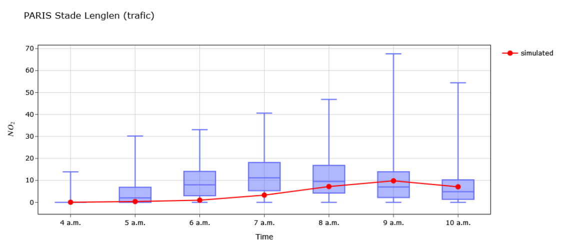

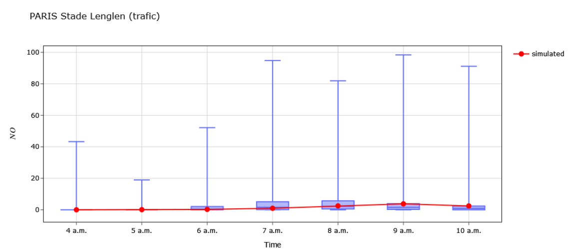

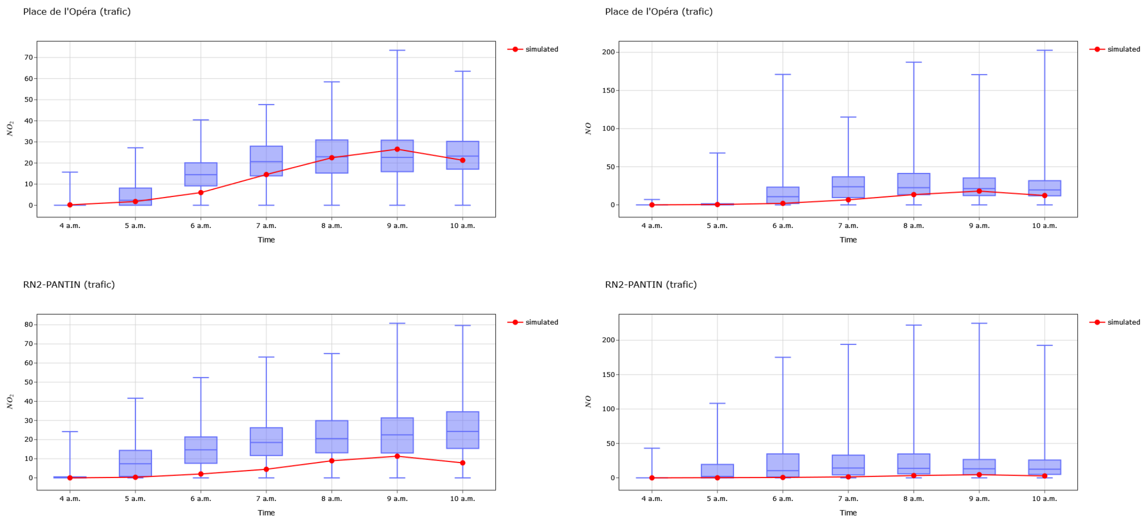

Figure 10: Observed concentrations of NO_2, NO in air pollution station in Île-de-France during 2021 compared with simulated values. Source: LCSQA and AirParif

Computation of economics costs of road traffic-related pollution with other methodology

In this annexe, we will explore alternative methodologies for monetizing air pollution linked to road traffic. One such approach, as proposed by Essen et al. (2019), involves determining the economic costs of air pollution from road traffic by considering average marginal costs per kilometer (€$.km^{-1}$) and per unit of emitted pollutants (€$.kg^{-1}$). The aim of this appendix is to juxtapose our methodology with conventional approaches found in the economics literature.

This table presents the results of the policy evaluation using two additional methodologies. Initially, our methodology indicates that in the "without mode choice" scenario, both environmental and health costs of pollution decrease by approximately -0.2% and -1.7%, respectively. In contrast, in the "with mode choice" scenario, these costs decrease even further by around -5% and -13%. However, when employing average marginal costs per kilometer, a different trend emerges. In the "without mode choice" scenario, both health and environmental costs increase by approximately 5% due to the increase of the vehicle kilometers. Consequently, this methodology may leads divergent conclusions regarding the impact of the policy on environ-

Computation of economics costs of road traffic-related pollution with other methodologies

	Baseline	Without mode choice	With mode choice
Our methodology			
Environmental costs (in k€)	571	569	542
Health costs (in k€)	956	940	922
Total (in k€)	1,527	1,509	1,464
CE Delft per kilometers			
Environmental costs (in k€)	62	65	59
Health costs (in k€)	371	388	357
Total (in k€)	433	453	416
CE Delft per emitted quantities			
Environmental costs (in k€)	571	569	542
Health costs (in k€)	258 669	257 665	243 645
Total (in k€)	829 1240	826 1234	785 1187

mental and health costs.

Regarding the methodology employing average marginal costs per emitted unit, in the "without mode choice" scenario, the environmental costs computed using this approach decrease by approximately -0.2%, and the health costs decrease by around -0.5%. Conversely, in the "with mode choice" scenario, environmental costs decrease by about -5%, and health costs decrease by approximately -6%, indicating similar decreases to those observed in our methodology. However, it is noteworthy that the quantitative outcomes vary depending on the computation factor (rural versus metropolitan), with our estimates being slightly higher than these estimations.

Lastly, it is crucial to acknowledge that our methodologies can be applied to a broad spectrum of pollutants until concentration-response functions are available in the epidemiologic literature. Additionally, our model can compute chemical transformations of pollutants, which is vital for assessing policies like those involving electric vehicles. For example, since electric vehicles do not emit NO_x, it is imperative to account for the excess of O_3 resulting from its non-destruction by NO_x.